THE KINETIC THEORY OF THE SOLAR WIND AND ITS INTERACTION WITH THE MOON

Thesis by

David Henry Griffel

In Partial Fulfillment of the Requirements

For the Degree of

Doctor of Philosophy

California Institute of Technology

Pasadena, California

1968

(Submitted December 18, 1967)

ACKNOWLEDGMENTS

I wish to record my deep gratitude to Professor Leverett Davis, Jr., who suggested this problem, and guided its solution around numerous pitfalls. I have profited also from discussions with Bill Burke, and Dr. George Siscoe.

I am grateful to the Institute for financial support; the work was partly supported also from NASA Grant NsG 426.

ABSTRACT

Beyond about .1 A.U. from the sun, fluid mechanics is not a good approximation for the solar wind, because the collision frequency is low. Analysis of the particle dynamics shows that if there are no collisions beyond .1 A.U., then at the earth $T_{\|}/T_{\perp} = 35$; this is much greater than is observed. We study the effects of interactions by means of the Boltzmann equation. Solving it with Krook's collision term, we find that the temperature anisotropy observed by the Vela satellite requires each particle to make an average of 2 or 3 collisions between .1 and 1 A.U. The temperature averaged over direction roughly follows an adiabatic law, with $\gamma = 3/2$; γ tends to increase with distance. The theory predicts an excess of high-velocity particles, as is observed by Vela, even when the collision frequency is independent of velocity; but to produce an effect as strong as that observed requires a fairly strong velocity-dependence of the collision frequency.

We proceed to study the interaction of the wind with the moon, treated as a solid body, with neither magnetic field nor atmosphere, absorbing and neutralizing all incident particles. We construct an exact theory of the boundary layer between such a body and a plasma with a magnetic field parallel to the surface, valid when the plasma has no velocity towards the surface. The thickness of the layer is about two gyroradii, and the magnetic field rises across it according to the equation of pressure balance.

We then consider two-dimensional models of the complete wind-planet interaction, and show that in any steady two-dimensional flow, the plasma velocity must be tangential to the body. Then, using the model of the sheath constructed above, we show that there can be no steady flow at all around a finitely conducting cylinder.

Finally, we consider the magnetic fields induced by the interplanetary field inside the moon, taking account of its rotation. If the applied field is uniform, then in the steady state there is a constant axial field inside the sphere; near the surface there is a complex toroidal field, dying away to zero in the interior if the sphere is spinning rapidly. If the external field is non-uniform, there is a residual toroidal field throughout the sphere. If the diffusion time is longer than the time between reversals of the interplanetary field, then the moon will contain concentric shells of toroidal and axial fields, independently diffusing inwards.

TABLE OF CONTENTS

I. INTRODUCTION

The sun appears to the naked eye — and, under normal conditions, to the telescope — as a disc, with a very sharp boundary. We are led to think of it as a sphere of gas, of definite radius ($\simeq 7.10^5$ km), sitting in a vacuum, and for many purposes (including a large part of astrophysics) this is perfectly satisfactory. However, evidence of various kinds suggests that it is not the whole truth. Eclipse photographs show that the sun is surrounded by an extensive and tenuous outer atmosphere, the corona; its size and shape vary with the solar cycle, and it shows no definite termination. Indeed, observations from spacecraft have shown that interplanetary space is filled with gas, at least as far out as the orbit of Mars, and probably much farther. The interplanetary gas is essentially fully ionized, mostly hydrogen but partly helium; its density fluctuates, but is of the order of 5 ions/cc at the earth; and it is blowing away from the sun (which is why it is called the solar wind) with a velocity around 300-500 km/sec. (except when there is a storm, when it may be much faster).

One immediately wonders why there is a solar wind at all. The answer seems to be that it is a continuous thermal expansion of the corona, caused by energy fed into it from below. The gas expands so rapidly that it overcomes solar gravity and escapes, coasting outwards among the planets until it is stopped by the interstellar plasma. Reasonable quantitative models of the wind have been constructed

along these lines.

The next question one might ask is what happens when the wind meets the planets. On Earth it is blamed for many things, ranging from the weather (more precisely, the temperature of the upper atmosphere — see MacDonald, 1963), through magnetic storms, to earthquakes.* It is clearly a complicated matter. The complication is caused largely by the geomagnetic field; the internal structure of the magnetosphere is rather complicated, and a great deal of the detailed mechanism of the radiation belts, aurora, and so on, is still obscure. But the broad outlines of the interaction of the wind and the earth are now fairly clear. The solar wind flows around the magnetosphere much as in the familiar aerodynamical problem of supersonic flow around a blunt body.

We shall here examine some of the problems that arise when the wind interacts with unmagnetized planets and satellites. At first sight this looks simpler than the magnetosphere. One knows the shape of the body around which the wind flows, without having to solve a free-boundary problem. However, if the body is conducting, then there is an electromagnetic interaction combined with the fluid dynamics, and this causes difficulty. In the absence of observational information, it is hard even to guess at the general flow pattern, and there are many problems to be solved before we reach a general understanding of the interaction. This dissertation examines three of these problems.

---

*Sytinskiy, 1966. The reader should note that this theory is not universally accepted.

First, we must understand the solar wind itself. It is usually treated by fluid mechanics. However, spacecraft observations have shown that the pressure tensor in the wind is not at all what one expects for a gas in local thermodynamic equilibrium, and therefore will not obey an equation of state of the usual kind. In particular, it is anisotropic: the pressure parallel to the field is considerably greater than that perpendicular. This may be expected to affect the pattern of flow around planets; perhaps we can include it in a fluid-mechanical theory by deriving some sort of equation of state for an anisotropic gas. This is discussed in Chapter 2; we find that if the collision frequency is so low that the pressure is anisotropic, then it is usually impossible to describe the plasma by differential equations of the fluid-mechanics type. We therefore use the methods of kinetic theory to calculate the properties of the solar wind at the earth, and relate the observed anisotropy to the collision frequency in interplanetary space.

Although in general fluid mechanics is wrong when the mean free path is long, the theory of Chew, Goldberger, and Low[40] justifies (as is discussed in Chapter 2) the use of MHD to study the flow of the wind around planets, at least in a semi-quantitative way. In Chapter 3 we use this method on a model of the flow around the moon. We first construct a kinetic theory of the boundary layer at the surface of the moon; this provides a boundary condition which we then apply to the problem of the general flow pattern.

We find that the flow is strongly influenced by the electromagnetic field inside the moon. In Chapter 4 we study this field in more detail, and determine the magnetic field induced inside the rotating moon by the interplanetary field.

Conventions

Gaussian units are used throughout.

$\sim$ means is of the order of

$\simeq$ means is approximately equal to

$\propto$ means is proportional to

$\hat{}$ denotes a unit vector

(5) means equation (5) of the current chapter .

II. FREE EXPANSION OF THE SOLAR WIND

2.1 Introduction

In this chapter we study the large-scale flow of the wind, and try to find a suitable theoretical description for it. The classic model (Parker 1958a, 1963a) uses the equations of fluid mechanics; it has no difficulty in reproducing the observed gross average behavior of the wind. However, fluid mechanics is only an approximation to the real world, and we must ask whether the approximation is valid for the solar wind.

In order to find the conditions for the validity of fluid mechanics, we sketch in §2.2 the derivation of fluid equations from the basic kinetic theory. We find that beyond about .1 A.U. from the sun, it is a poor approximation. This was realized by Parker from the beginning; it does not much affect the validity of his results, since the equations break down only in a region where the solutions are more or less constant, and insensitive to the details of the equations. However, we shall see that going beyond the fluid approximation gives us useful information about the velocity distribution in the gas, which cannot be deduced from fluid mechanics.

As a first step in this direction, §2.3 studies the flow beyond .1 A.U., neglecting collisions. This assumption leads to the conclusion that the temperature parallel to the magnetic field near the earth is greater than the perpendicular temperature; this agrees with the observations, but the predicted anisotropy is far more than

is observed. This suggests that there are relaxation mechanisms at work in the wind (as is expected on other grounds). Accordingly, in §2.4 we examine the Boltzmann equation including interactions, and formulate a well-posed problem for it. In §2.5 we present the results of numerical solutions of the Boltzmann equation, with Krook's form of the collision term. Some general remarks about the validity of our calculation are made in §2.6.

Before embarking on this program, we must state precisely what we mean by the parallel and perpendicular temperatures.

The Definition of Temperature

The thermodynamic definition of temperature applies only to systems in equilibrium. The word temperature has not been used very much for non-equilibrium systems, and we are therefore at liberty to define it in any (reasonable) way that we please, as long as it agrees with the usual definition for systems in equilibrium. Now, for a dilute gas in equilibrium, with pressure p, temperature T, and number density n, the temperature is related to the pressure by $p = nkT$. For a non-equilibrium gas, it is conventional to define a pressure tensor $p_{ij}(x) = \rho \langle c_i c_j \rangle$; ρ is the mass density, and $\langle c_i c_j \rangle$ is the average (over the velocity distribution) of the product of peculiar velocities $\underset{\sim}{c}$, defined as the difference between the velocity of a particle at the point x and the mean velocity of the whole gas at that point (see Chapman and Cowling 1952). By analogy with the equilibrium case, we shall define the temperature in general to be a tensor proportional to the pressure tensor:

$$T_{ij} = \frac{1}{nk} p_{ij} = \frac{m}{k} < c_i c_j > \quad .$$

The three diagonal components T_{ii} are directly proportional to the spread in velocity (squared) along the three axes. For a plasma in a strong magnetic field, in the z direction, say, T_{xx} and T_{yy} involve the gyratory velocities, and are therefore equal, since those velocities are symmetrical about the z axis.* In coordinates aligned with the field, the temperature tensor takes the form

$$\begin{pmatrix} T_\perp & & 0 \\ & T_\perp & \\ 0 & & T_\parallel \end{pmatrix} \quad .$$

For a gas in equilibrium, $T_\perp = T_\parallel = T$, where T is the usual definition of temperature.

We should remark that a different definition of temperature is sometimes used in the analysis of observational data: one constructs a theoretical velocity distribution function by multiplying Gaussian distributions for each velocity component, with different 'temperatures' along the three axes; one then adjusts T_i to fit the theoretical distribution to the observed data. The three T_i are then called the tempera-

---

*This may be false if there is some peculiar correlation between the phases of the gyrations of all the particles; but even then it is true if T is averaged over a gyroperiod.

tures along the three axes. Clearly, if the true distribution is in fact a product of Maxwellians, then the two definitions agree; and they are not likely to differ widely unless the distribution is very peculiar.

2.2 Kinetic Theory and Fluid Mechanics

The only equations for the solar wind in which we may have unbounded confidence are Newton's laws, written down for each particle individually. This is, of course, an impossibly complicated set of equations, and gives far too detailed a description of the state of the gas. As is usual in problems of this kind, we shall introduce the one-particle distribution function f : $f(x,v,t)$ is the number of particles in the element $d^3x d^3v$ of phase space, at time t. It does not give a complete description of the state of the gas, since it says nothing about the correlations between the particles; but it contains more than enough information for our present purposes.

If there are no interactions between the particles, then we do not expect correlations to be important. In this case we can indeed find an equation which determines the one-particle distribution f completely, and without mention of the many-particle joint distributions. Newton's laws imply that f is constant along particle trajectories in phase space (this is Liouville's theorem — see, for example, Goldstein's 'Classical Mechanics'). Hence, if $\underset{\sim}{F}$ is the external force on the system,

$$\frac{\partial f}{\partial t} + \underset{\sim}{v} \cdot \frac{\partial f}{\partial \underset{\sim}{x}} + \frac{1}{m} \underset{\sim}{F} \cdot \frac{\partial f}{\partial \underset{\sim}{v}} = 0 \ . \qquad (2\text{-}1)$$

Given f at any time, this equation is easily solved to give f at all future times. It has the form of a conservation law in $(\underset{\sim}{x},\underset{\sim}{v})$ space, which is not quite the same as the $(\underset{\sim}{x}, \underset{\sim}{p})$ phase space. But since the volume elements are equal (up to a factor of m), phase space may be replaced by $(\underset{\sim}{x},\underset{\sim}{v})$ space for our purposes.

If the particles interact, then the external force field $\underset{\sim}{F}$ is not the total force on the particles, and (1) is no longer true. However, one may derive from Newton's laws the equation

$$\frac{\partial f}{\partial t} + \underset{\sim}{v} \cdot \frac{\partial f}{\partial \underset{\sim}{x}} + \frac{1}{m} \underset{\sim}{F} \cdot \frac{\partial f}{\partial \underset{\sim}{v}} = C , \qquad (2\text{-}2)$$

where C is determined by a set of (N - 1) equations involving the (N - 1) higher joint distribution functions.* It is, of course, impracticable to find C by solving those equations — that would be equivalent to solving Newton's equations for the N-particle system. The usual procedure is to ignore the higher equations, and find an approximation to C by independent physical arguments.

If there are no interactions, then f satisfies (1); comparing (1) and (2), we see that C represents the effects of collisions upon the evolution of the gas. We shall refer to (2), for any choice of the collision term C, as the Boltzmann equation (the equation that Boltzmann himself used was based upon a particular approximation for

---

*This is the Bogoliubov-Born-Green-Kirkwood-Yvon system of equations; a discussion and references will be found in Shkarofsky et al., 1966.

C; it may be referred to as Boltzmann's Boltzmann equation when there is danger of confusion).

Let us lay aside for the present the problem of calculating C, and consider how one can use (2) for solving problems in gas dynamics. It is still very hard to solve a boundary-value problem for this equation, with any reasonably realistic form of the collision term; and it would still give us much more information than we need. We are interested mainly in the density, velocity, and temperature of the gas, rather than the finer details of the distribution. This gives the clue to the usual method of handling fluid-mechanical problems: the density, velocity, and temperature are respectively the zeroth, first, and second velocity moments of f (the nth moment means the nth rank tensor $\int d^3v\ f(x,v)\ v_i v_j \ldots v_p$). We can try to work directly with the moments of f instead of with f itself, and hope to be able to determine the first few moments without having to discuss the higher ones.

We may derive a set of equations involving only the moments of f, by taking moments of the Boltzmann equation — that is, by multiplying it by various powers of $\underset{\sim}{v}$ and then integrating. By itself, of course, this process does not make the problem any easier. It gives an infinite set of coupled equations; the nth determines the (n+1)th moment in terms of the nth and higher moments. However, in this form the problem suggests an approximation-method: if we can somehow truncate this sequence of equations, we will be left with a finite set of differential equations in $\underset{\sim}{x}$ space (the velocity variables

have been eliminated by the device of taking moments).

The first member of the set of moment equations relates the density to the velocity; it is the continuity equation. The second is the momentum equation: it relates the velocity to the divergence of the pressure. The pressure is determined in terms of the higher moments by the third equation, and so on. If there were an independent way of determining the pressure without using the third and higher moments, then the continuity and momentum equations would be a closed system, from which the velocity and density fields could be determined. This is precisely the method of fluid dynamics, and it is the method which most successful treatments of the solar wind have used.

We must now discuss when and how the pressure can be determined without use of the higher moments of the distribution function. The usual arguments (see Chapman and Cowling) apply to gases in which there are many collisions — the mean free path and collision time are much smaller than the characteristic length and time of the problem. This means that each little piece of gas is locally in thermodynamic equilibrium at all times, since the time it takes for a gas to come to equilibrium is of the order of a collision time. A gas in equilibrium satisfies an equation of state: the pressure is determined in terms of the density and temperature; and the temperature is determined by energy conservation. Thus the equation of state, combined with the continuity, energy, and momentum equations, completely determines the problem; the Navier-Stokes equations are valid for collision-dominated gases.

This situation may be described in slightly different words. In general, the distribution function may be an arbitrary function of velocity; if it is to be described by its moments, it takes an infinite number of moments to specify f(v). But if there are so many collisions that the gas is locally in statistical equilibrium, then the distribution function must be Maxwellian: it loses most of its freedom, and may be described completely by only a few parameters. It is thus very reasonable that the gas can be discussed completely in terms of the first few moments of f.

Now let us consider what happens when the collision frequency is not high. Then the velocity distribution is not constrained to be Maxwellian, but can be an arbitrary function; it therefore seems unlikely that we can truncate the sequence of moment equations, and describe the gas by its first few moments only. When the mean free path is long, the molecules can travel more or less freely through the gas. At any point there are always some particles which have just arrived from distant parts; their properties depend upon the velocity distribution at those distant places. Therefore there can be no local equation of state, and nothing resembling the Navier-Stokes equations: the state of the gas at any point depends not only on the state at neighboring points, but also on the state at distant points, and so a description in terms of differential equations in x-space is impossible. For rarefied gases, it seems that one must abandon the moment equations, and start afresh from the Boltzmann equation.

There is one well-known exception to this rule, and that is a plasma in a strong magnetic field. If the gyroradius is smaller than the scale length of the problem then the motion of the particles across the field is severely restricted. Therefore the argument given above for the nonexistence of a local equation of state breaks down. Chew, Goldberger, and Low (1956)* have in fact shown that under certain conditions a collisionless plasma in a strong magnetic field satisfies a set of equations of the fluid type. However, the field restricts the motion only across the field; particles can move freely along it. Therefore we cannot expect fluid behavior in cases where the motion is mainly along the field. The CGL equations apply only when the motion along the field is in some sense trivial — as, for example, in two-dimensional problems. To study the interaction of the wind with the earth, it is reasonable to consider a model in which the field is perpendicular to the velocity of the wind (in fact, the angle is about 45°). We then expect the wind to behave like a fluid, as long as the gyroradius is smaller than the scale length; and this is confirmed by observations (see Ch. 3). On the other hand, the general large-scale expansion of the solar wind is essentially a flow along the field, and so the CGL theory does not apply.

Now that we have surveyed briefly the derivation of fluid equations from the fundamental kinetic theory, we can ask if and when such equations are valid for the solar wind. If we take the observed

---

*See also Bernstein and Trehan, 1960, and Parker, 1957.

properties of the wind near the earth, and compute the effective mean free path for Coulomb collisions (using the formula in Spitzer's book, for example), we find that it is longer than 1 A.U. ($\simeq 1.5.10^8$ km.). So collisions are completely negligible near the earth. There is little direct information on conditions closer to the sun. But there are fluid models (Parker 1963a) which predict the temperature, velocity, and density of the wind down to a few solar radii; we can take those predictions, compute the collision mean free path, and ask if it is short, as it must be to make the fluid model consistent. The answer is that below about 20 solar radii, the mean free path is short compared to the scale length, and fluid mechanics is correct; but beyond this distance the collision rate drops off very sharply, and Coulomb collisions are negligible.

Thus we are not entitled to assume the validity of fluid mechanics beyond about .1 A.U. from the sun. We must return to the Boltzmann equation.

2.3 Collisionless Dynamics

In this section we shall study the dynamics of particles moving through the interplanetary field without any collisions, either with particles or with waves — we assume the magnetic field is smooth. Even though interactions may be important in the solar wind, we must understand the free-particle dynamics before going on to more realistic calculations. We shall suppose that the wind is collision-dominated up to .1 A.U., and collisionless beyond. Since the Coulomb collision frequency in fact drops off quite sharply with distance, this is a good approximation. To display the phenomena in their simplest form we shall first briefly consider a model which ignores the rotation of the sun and the curvature of the interplanetary field, and then take these effects into account.*

We consider, then, the motion of particles in a radial magnetic field. Since the gyroradii are much smaller than the scale length of the field (which is of the order of the distance from the sun), the adiabatic approximation to the orbits is valid. The particles move out along field lines, conserving both their energy and their magnetic moment (defined as $W_\perp/B$, where B is the magnetic field, and $W_\perp = \frac{1}{2}mv_\perp^2$ is the gyration energy). As they move outwards through the inverse-square field, $W_\perp$ decreases in proportion to B, and therefore $T_\perp$, which

---

*The simplest model of all ignores both collisions and magnetic fields. Even though neglect of the field seems unjustifiable, this model has some interesting properties; it is discussed in Appendix A.

is proportional to $W_\perp$, decreases also.

Now, the energy is conserved, and so the parallel velocity $v_\parallel$ must increase when $v_\perp$ decreases. In fact, $v_\parallel^2 + v_\perp^2 = \text{const.}$ (solar gravity is negligible at these distances), so $d(v_\parallel^2) + d(v_\perp^2) = 0$. But $v_\parallel^2 \gg v_\perp^2$ in the solar wind; therefore the fractional change in $v_\parallel^2$ is small even when $v_\perp$ decreases by a large factor. So $v_\parallel$ is approximately constant as the plasma moves outwards. Thus $T_\parallel$ will be roughly constant, while $T_\perp$ decreases in proportion to the magnetic field. If the dynamics were truly collisionless beyond .1 A.U., and the sun did not rotate, then near the earth the plasma would be extremely anisotropic, with $T_\parallel/T_\perp \simeq 100$.

Motion in a Spiral Field

We shall now allow the sun to rotate. Its magnetic field becomes twisted into the familiar spiral pattern, but the general character of the windflow is not much affected. One might not expect much change in the particle motions, except for a rotation of the plane of gyration as the particle follows the curved B lines, and perhaps some adiabatic drifts. However, it turns out that the anisotropy is reduced by a factor of three, compared with the radial field case. To show this, we must devote several pages to a detailed study of the particle dynamics in the spiral field.

The magnetic field pattern is well known (Parker 1963b): on the sun's equatorial plane, the angle ψ between the field and the radial direction is given by

$$\tan \psi = \frac{r}{R} \quad , \qquad (2\text{-}3)$$

where r is the distance from the sun, and R is a constant, $\simeq$ 1 A.U.; $R = V/\Omega$, where V is the bulk velocity of the solar wind and Ω is the solar rotation frequency. The radial component $B_r \propto 1/r^2$ (this follows from div $\underset{\sim}{B} = 0$, assuming spherical symmetry near the equatorial plane); and so the field strength is

$$B = \frac{B_0 \sec \psi}{r^2} , \qquad (2\text{-}4)$$

where B_0 is a constant.

The theory will be restricted to the solar equatorial plane, since that is where all the observations are being made (we ignore the small angle between the ecliptic and equatorial planes). We shall suppose that the magnetic field points outwards from the sun; the final results, of course, will not depend upon its sign.

Now, (3) is true if the bulk velocity of the wind is constant and radial. Since the magnetic energy density in the solar wind is much less than the kinetic energy density, one does not expect the radial flow to be much affected by the field; and observations show that the windflow is indeed close to radial. The particles are therefore not moving strictly along the spiral field lines, but drifting across them as well. There must therefore be an electric field, perpendicular to $\underset{\sim}{B}$ and to the drift speed, and hence in the North-South direction. Now, it is observed that the thermal speeds in the solar wind are much less than the bulk speed; so practically all the particles are traveling with radial velocity close to V. We resolve the guiding-center velocity into components: u along the field, and v_D perpendicular to it and in

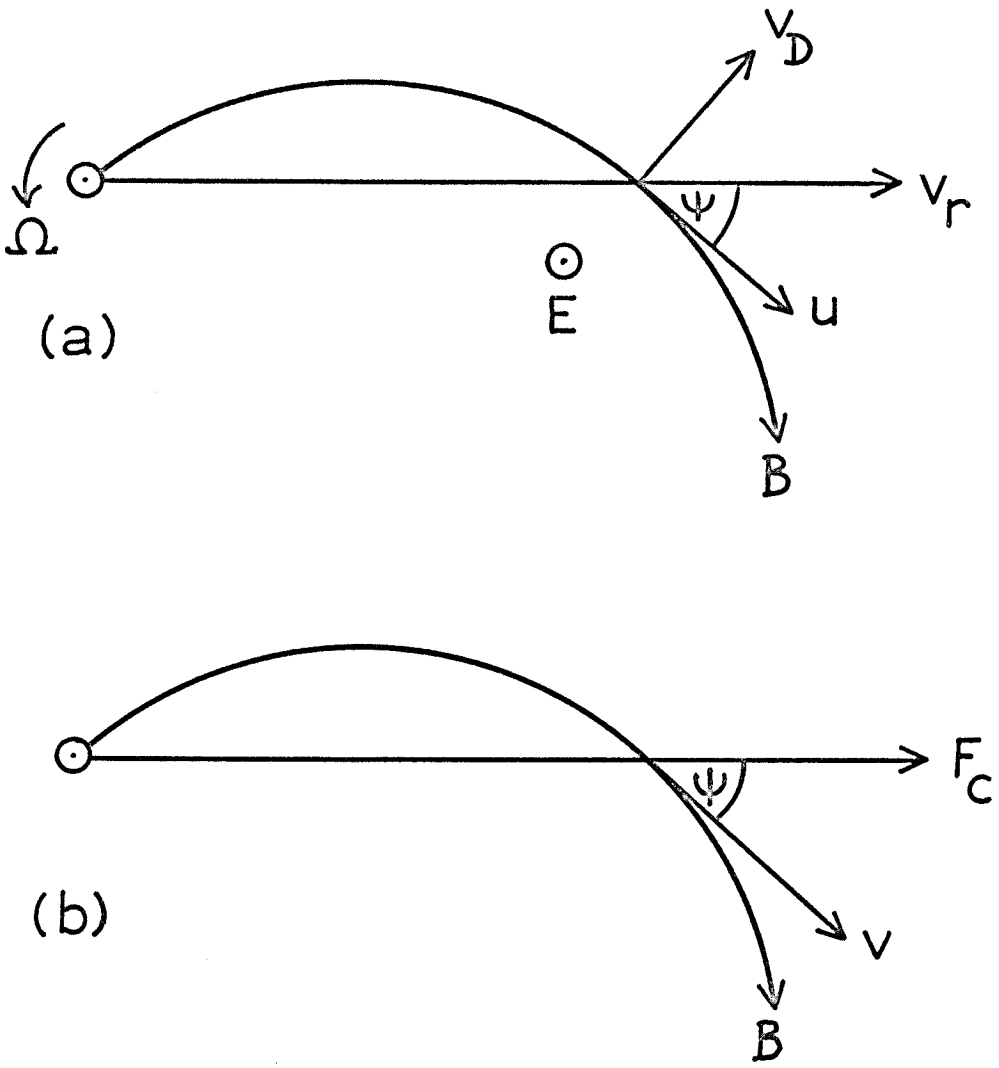

Figure 1. Particle Dynamics in the Solar Wind

(a) The fixed frame

(b) The rotating frame

the ecliptic plane (there is a third component, out of the ecliptic, but it is much smaller). For a particle whose guiding center is traveling radially with speed V,

$$v_D = V \sin \psi \tag{2-5}$$

(see Fig. 1a). This is an $\underset{\sim}{E} \times \underset{\sim}{B}$ drift; therefore $V \sin \psi = cE/B$ and

$$E = \frac{VB}{c} \sin \psi \ . \tag{2-6}$$

This is the Northwards electric field needed to produce the azimuthal drift. Using (3), it may be rewritten

$$E = \frac{\Omega r}{c} B \cos \psi \ .$$

This is a very reasonable result: it means that in a frame traveling with the local solar rotation speed $r\Omega$, there is no electric field; in other words, the interplanetary magnetic field lines rotate with the sun.*

We shall now consider in detail the motion of particles in the field defined by (3) and (6): we are interested in the small deviations from perfectly radial flow with speed V. The invariance of the magnetic moment implies that the gyration energy $\frac{1}{2}mv_\perp^2$ is proportional to B (note that $v_\perp$ is defined not as the component of the particle

---

*Notice that this is not an extra assumption, but an immediate consequence of supposing that the flow is essentially collisionless and radial.

velocity perpendicular to the field, but as the velocity of gyration, which is the difference between that component and the electric drift speed). Because there is an electric field, the kinetic energy is not conserved, and the calculation of the parallel velocity u is not so easy.

The magnetic field is curved, and the electric field is space-dependent; therefore, the particles will drift slowly Northwards, and thus gain or lose energy from the electric field, depending on the sign; the energy equation is

$$v_r \frac{d}{dr} \left[\frac{m}{2} (u^2 + v_\perp^2) \right] = eEv_z \quad .$$

The drifts are all small, and make a negligible contribution to the kinetic energy. E is known; and v_z may be calculated by adding: (a) the gradient $\underset{\sim}{B}$ drift, (b) the curvature drift, and (c) the mixed drift. This last is a drift which occurs when there are space-dependent magnetic and electric fields both present (Northrop 1961); it may be thought of as an acceleration drift caused by the change in the $\underset{\sim}{E} \times \underset{\sim}{B}$ drift speed. All these drifts can be computed, and the resulting equation of motion solved. It is a lot of hard work.

However, the same result may be reached with very much less labor by working in a coordinate system rotating with the sun, for there is no electric field in that frame. Since it is not an inertial frame, it is not immediately obvious what the equations of electromagnetism are. We must start from the known equation of motion in the

inertial frame:

$$m \frac{d\underset{\sim}{u}}{dt} = e(\underset{\sim}{E} + \underset{\sim}{u} \times \underset{\sim}{B}/c) \ .$$

Now we make a coordinate transformation to the rotating axes, writing $\underset{\sim}{u} = \underset{\sim}{v} + \underset{\sim}{U}_R$, where $\underset{\sim}{U}_R = \underset{\sim}{\Omega} \times \underset{\sim}{r}$ is the rotation speed. Then we have

$$m \frac{d\underset{\sim}{v}}{dt} + \underset{\sim}{I} = e(\underset{\sim}{E} + \underset{\sim}{U}_R \times \underset{\sim}{B}/c + \underset{\sim}{v} \times \underset{\sim}{B}/c) \ ,$$

where the inertial force $\underset{\sim}{I}$ (centrifugal + Coriolis) comes from transforming the time-derivative in the usual way. But $\underset{\sim}{E} + \underset{\sim}{U}_R \times \underset{\sim}{B}/c$ is the familiar Lorentz transformation formula. Thus we have shown that if the electromagnetic fields are transformed by the prescription $\underset{\sim}{E}' = \underset{\sim}{E} + \underset{\sim}{U}_R \times \underset{\sim}{B}/c$, $\underset{\sim}{B}' = \underset{\sim}{B}$, and if $U_R = r\Omega \ll c$, then the equation of motion in rotating axes is given correctly by the Lorentz force law, plus centrifugal and Coriolis forces.

The Coriolis force is $2m\underset{\sim}{v} \times \underset{\sim}{\Omega}$, which closely resembles the magnetic force. In fact, if we define $\underset{\sim}{C} = 2mc\ \underset{\sim}{\Omega}/e$, then the equation of motion is

$$m \frac{d\underset{\sim}{v}}{dt} = \frac{e}{c} \underset{\sim}{v} \times (\underset{\sim}{B} + \underset{\sim}{C}) + m\Omega^2 \underset{\sim}{r} \ . \qquad (2\text{-}7)$$

The Coriolis force behaves exactly like an additional magnetic field $\underset{\sim}{C}$, pointing North. It is a small perturbation on $\underset{\sim}{B}$, since $\Omega \ll \omega = eB/mc$; indeed, $\Omega/\omega \sim 10^{-5}$. So in this frame, to a first approximation, the guiding centers move along magnetic field lines, with a small Northwards velocity corresponding to the North component of the "total field" $\underset{\sim}{B} + \underset{\sim}{C}$. There are other drifts produced by the curvature and gradient

of the field, but these are all smaller than the parallel velocity by at least a factor $(\Omega/\omega) \sim 10^{-5}$. They make a negligible contribution to the kinetic energy; and since there is no electric field in this frame, they do not contribute anything to the total energy.

The last term of (7) is the centrifugal force F_c. Its component perpendicular to the magnetic field produces a small perpendicular drift, again negligible; but its component along the field accelerates the particles. If v is the guiding-center velocity in the co-rotating frame, then the radial velocity is

$$v_r = v \cos \psi \tag{2-8}$$

(see Fig. 1b). So the work per second performed on the particle by the centrifugal force is $v_r . m\Omega^2 r$, and the energy equation is

$$\frac{d}{dt} \frac{m}{2} (v^2 + v_\perp^2) = v_r \frac{d}{dr} \frac{m}{2} (v_2 + v_\perp^2) = m\Omega^2 r \, v_r;$$

hence

$$v^2 = \Omega^2 r^2 + A - v_\perp^2$$

where A is a constant of integration. But $v_\perp^2 \ll \Omega^2 r^2$ in the solar wind; $\Omega^2 r^2$ is the term dominating the r-dependence of v, and we may write, to a good approximation,

$$v^2 = \Omega^2 r^2 + A. \tag{2-9}$$

We must now relate v to u, the parallel velocity in the inertial frame. Clearly, the radial velocity v_r is the same in the two frames; therefore we find

$$v = u + \Omega \, r \sin \psi \, .$$

(9) now becomes

$$(u + \Omega r \sin \psi)^2 = \Omega^2 r^2 + A. \tag{2-10}$$

This gives u as a function of r.

To complete the solution of the dynamics, we determine $v_\perp$ from the invariance of the magnetic moment, which implies

$$v_\perp^2 \propto B \propto \frac{\sec \psi}{r^2} = \frac{\sqrt{1 + r^2/R^2}}{r^2} \quad . \tag{2-11}$$

Now, $T_\perp \propto < v_\perp^2 >$; therefore

$$T_\perp \propto B \propto \frac{\sqrt{r^2 + R^2}}{r^2} \quad . \tag{2-12}$$

Thus the perpendicular temperature falls off rapidly with distance, though not quite so rapidly as if the field were strictly radial and inverse-square.

The parallel temperature is no longer constant, as it was when the field was radial. Consider u as a function of r and the initial value U = u(r = D), where r = D = .1 A.U. is the starting-point of our calculation. From (10),

$$u = \sqrt{\Omega^2 r^2 + A} - \Omega r \sin \psi,$$

where

$$A = (U + \Omega D \sin \psi)^2 - \Omega^2 D^2 \quad .$$

If two particles differ in velocity by δU at r = D, then at r they differ in velocity by $\delta u = (\partial u/\partial U) \cdot \delta U$. Now,

$$\frac{\partial u}{\partial U} = \frac{\partial u}{\partial A}\frac{dA}{dU} = \frac{U + \Omega D \sin\psi}{\sqrt{\Omega^2 r^2 + A}} \quad .$$

To a first approximation, U = V, the mean solar windspeed. So

$$\frac{\partial u}{\partial U} = \left[1 + \frac{r^2 - D^2}{(R + r\,D/\sqrt{r^2 + R^2})^2} \right]^{-\frac{1}{2}} ,$$

using (3).

Now, $T_{\|} \propto (\delta u)^2 \propto (\partial u/\partial U)^2$; so

$$T_{\|} = T_{\|}^{D} \left[1 + \frac{r^2 - D^2}{\left[R + rD/\sqrt{R^2 + r^2}\right]^2} \right]^{-1} \qquad (2\text{-}13)$$

where the constant $T_{\|}^{D} = T_{\|}$ (r = D). In our case, D = .1 A.U., so R = r = 10D at the earth, so $T_{\|} \simeq \frac{1}{2} T_{\|}^{D}$. Thus the parallel temperature decreases as well as the perpendicular temperature, but rather more slowly (in the collisionless theory).

If we suppose that the distribution is isotropic at .1 A.U., and the flow is collisionless from there onwards, then near the earth $T_{\|}/T_{\perp} \simeq 35$. This is extremely anisotropic; on theoretical grounds it seems unlikely that it will really occur. There are observations of the velocity distribution in the solar wind from the Pioneer 6 and Vela 3 satellites (Scarf et al., 1967, Hundhausen et al., 1967). They find that the distribution is indeed anisotropic, and the anisotropy is aligned with the magnetic field, but the temperature ratio is only 1.5 - 4. Therefore the collisionless model is inadequate; there

must be relaxation processes at work, trying to drive the distribution towards an isotropic Maxwellian. The rest of this chapter studies these effects.

The Liouville Equation

In preparation for the next section, we shall now derive an equation for the distribution function in the collisionless theory; it is an expression of Liouville's Theorem. This theorem (which follows from Newton's laws alone) says that the distribution function is constant along particle trajectories in phase space. The mathematical expression of this statement is equation (1); when, as in our case, the only forces are electromagnetic, (1) reads

$$\frac{\partial f}{\partial t} + \underset{\sim}{v} \cdot \frac{\partial f}{\partial \underset{\sim}{x}} + \frac{e}{m}\left(\underset{\sim}{E} + \frac{1}{c}\,\underset{\sim}{v} \times \underset{\sim}{B}\right) \cdot \frac{\partial f}{\partial \underset{\sim}{v}} = 0 \quad . \tag{2-14}$$

(Even though we are using noncanonical coordinates $(\underset{\sim}{x}, \underset{\sim}{v})$ in phase space, the conservation equation (14) is true.) It looks fairly complicated. Therefore we shall transform to a new set of coordinates in phase space, such that the Liouville equation simplifies.

If $\underset{\sim}{x}$ and $\underset{\sim}{v}$ are given, then the acceleration is determined by Newton's laws, and thus the direction of motion of the particles in phase space is determined. Through each phase point, then, there passes a unique orbit curve: phase space is completely filled with a family of these trajectories (they are the characteristic curves of the partial differential equation (14)). Instead of describing a point by its coordinates $(\underset{\sim}{x},\underset{\sim}{v})$, we shall describe it by saying (a) which

trajectory it is on, and (b) how far along that trajectory it is, measured from some standard reference point.* If s is the coordinate along the trajectory (it may or may not be linear with distance), then the Liouville equation is simply

$$\frac{\partial f}{\partial s} = 0 \quad .$$

This is trivially solved: f = A, where A is an arbitrary function of the five variables which label the trajectories. This is all excessively simple, of course, but we are developing the machinery because it will be useful when we come to consider the effect of collisions, in §2.4.

We must now describe our new coordinate system in detail. First we shall make a transformation in velocity space which removes the electric drift. We define

$$\underset{\sim}{v}' = \underset{\sim}{v} - \underset{\sim}{v}_D \quad ,$$

where $\underset{\sim}{v}_D$ is the $\underset{\sim}{E} \times \underset{\sim}{B}$ drift speed. This transformation leaves the volume element in phase space invariant; therefore if $f(x,v')d^3xd^3v'$ is the number of particles in the box $d^3 \times d^3v'$, then f is constant along orbits, as before. We shall use cylindrical coordinates in velocity space, with v_z' directed along the local magnetic field; then $v_z' = u$, the parallel velocity, and $v_\perp$ is the r-component in the

---

*These are the characteristic coordinates commonly used for solving hyperbolic partial differential equations.

cylindrical coordinate system.

The orbit curves are described by (9), (10). These equations involve only three dimensions of the six-dimensional phase space. We assume that the distribution function is independent of the three angular variables: θ and φ in x-space, and the phase angle ψ in velocity space; then there is no need to explicitly consider those variables, and we may work in a three-dimensional reduced phase space, with axes r, u, $v_\perp$. We can now uniquely label the orbits by the values U, $V_\perp$ of u, $v_\perp$ at a reference point r = D; and r measures distance along the orbit. The old coordinates u and $v_\perp$ are given as functions of r and U, $V_\perp$ by (8), (9):

$$v_\perp^2 = \frac{B(r)}{B(D)} V_\perp^2 \tag{2-15}$$

and

$$u = \sqrt{A + \Omega^2 r^2} - \Omega r \sin \psi , \tag{2-16}$$

where

$$A = (U + \Omega D \sin \psi)^2 - \Omega^2 D^2 .$$

The Liouville equation is now

$$\left(\frac{\partial f}{\partial r}\right)_{U,V_\perp} = 0 . \tag{2-17}$$

2.4 Collision Effects

We shall now extend the theory of §2.3 to include relaxation effects. Coulomb collisions are negligible in the region that we are considering; but there are magnetic interactions between the particles. Observations show that the magnetic field is irregular on a small scale; indeed, plasma theory* predicts that if the distribution is considerably anisotropic (as is suggested by the results of §2.3), then the plasma is unstable, and waves are generated; the field lines become crinkly. Particles bounce off these magnetic kinks in much the same way as they bounce off other particles, and the general effect, like that of all interaction processes, is to drive the system towards a Boltzmann distribution.

In order to be able to treat the process mathematically, we shall at first take a specific model for the collisions: we suppose that they produce sudden random changes in the velocity of the particles; the velocity vector thus performs a random walk. If the magnetic field may be considered static over the time of a collision, then energy is conserved, so the random walk is restricted to a two-dimensional constant-energy surface in velocity space. We further suppose that the particles suffer many small deflections, rather than a few large ones, so that the random walk may be treated as a quasi-continuous process, and described by a differential equation of the diffusion type.

---

*Parker, 1958b.

Finally we assume that the scattering is isotropic in velocity* — within the restrictions of energy conservation. We thus have an isotropic random walk on the surface of a sphere in velocity space. These assumptions are made here only for the sake of having a definite model to discuss; there will be no such restriction on the validity of the equation which we shall eventually use in §2.5 to describe the solar wind.

We have now completely specified the scattering process, and should therefore be able to compute the collision term of Boltzmann's equation. This is discussed by Chandrasekhar (1943); Boltzmann's equation for a random walk with small step sizes is called the Fokker-Planck equation, and in our case is

$$\frac{Df}{Dt} = \frac{\sigma^2}{4} \frac{\partial}{\partial \mu} \left[(1-\mu^2) \frac{\partial f}{\partial \mu} \right] , \qquad (2\text{-}18)$$

where f is the distribution function, μ is the cosine of the angle between the velocity vector and the magnetic field, and $\tau\sigma^2$ is the mean square step size if steps are taken once every τ seconds; D/Dt is the operator on the left side of (14).

Properties of the Fokker-Planck Equation

As $\sigma \to 0$, (18) becomes the Liouville equation (14). The solution of this is a step-by-step procedure: starting with some

---

*We shall see later that this is not a good assumption. We make it because it leads to a simple equation, whose properties are easy to understand; the conclusions we shall reach are valid also for the more accurate equation solved in §2.5.

assumed distribution near the sun, one can deduce the distribution farther out. It seems reasonable that if we know the state of the plasma near the sun, then we should be able to integrate outwards to find its distribution function at the earth. However, we shall see that this is not necessarily true.

We shall consider the Fokker-Planck equation in a constant magnetic field, and in a steady state:

$$\mu \frac{\partial f}{\partial x} = \frac{\sigma^2}{4V} \frac{\partial}{\partial \mu} \left[(1-\mu^2) \frac{\partial f}{\partial \mu} \right] , \qquad (2\text{-}19)$$

where V is the speed of the particle, which is invariant. This looks very much like the diffusion equation in spherical coordinates:

$$\frac{\partial f}{\partial t} = k \frac{\partial}{\partial \mu} \left[(1-\mu^2) \frac{\partial f}{\partial \mu} \right] . \qquad (2\text{-}20)$$

x is the "timelike" variable. The initial-value problem is certainly well-posed for the diffusion equation (20), just as it is for the Liouville equation. However, (20) differs from the Liouville equation in being irreversible. If one prescribes f arbitrarily at $t = 0$, say, and k is positive, then for all $t < 0$ the equation has a unique and finite solution. But if one tries to use the equation to find f for $t < 0$ ("solving it backwards in time"), one finds that the solution fluctuates more and more wildly, and there is a finite time -T beyond which it cannot be continued. The diffusion equation can only be solved forwards in time.

Now, changing the sign of k in (20) is equivalent to changing the sign of t. Hence, if $k < 0$, (20) can only be solved backwards in t.

But in the Fokker-Planck equation (19), the coefficient μ changes sign; hence (19) is a parabolic (i.e., diffusionlike) equation for $\mu > 0$ and for $\mu < 0$, but "time" runs in opposite directions in these two regions. For $\mu > 0$ it can indeed be solved forwards in x, but for $\mu < 0$ it can only be solved backwards in x. These two requirements are incompatible, for the equation (19) links the two regions. Therefore, in order to solve (19) for $\mu > 0$ forwards in x, one must first have found $f(\mu < 0)$ by integrating backwards in x; and vice versâ.

To clarify this confusing situation, consider Figure 2, which depicts the relevant dimensions of phase space. All particles with $\mu > 0$ (pitch angle $< \pi/2$) are moving in the +x direction, with speed $V\mu$; those with $\mu < 0$ are moving in the -x direction. Superimposed upon this directed flow is a random walk in the μ-direction. It is now easy to see that the initial-value problem is ill-posed. Suppose, for example, that one prescribes $f(x = 0, \mu > 0)$, and demands $f(0, \mu < 0) = 0$. Now, $f(0, \mu > 0) > 0$ means that particles are entering the diagram at the upper left side, traveling to the right. Some of them will be knocked into the lower half of the diagram by collisions; of course, some of those will later be kicked back up again, and there will be a continuous circulation of particles in phase space. Inevitably, however, some particles will arrive back at $x = 0$ in the lower half plane, thus killing off all hope of satisfying $f(0, \mu < 0) = 0$.

Suppose that we wish to solve (18) over the range $0 \leqslant x \leqslant X$.

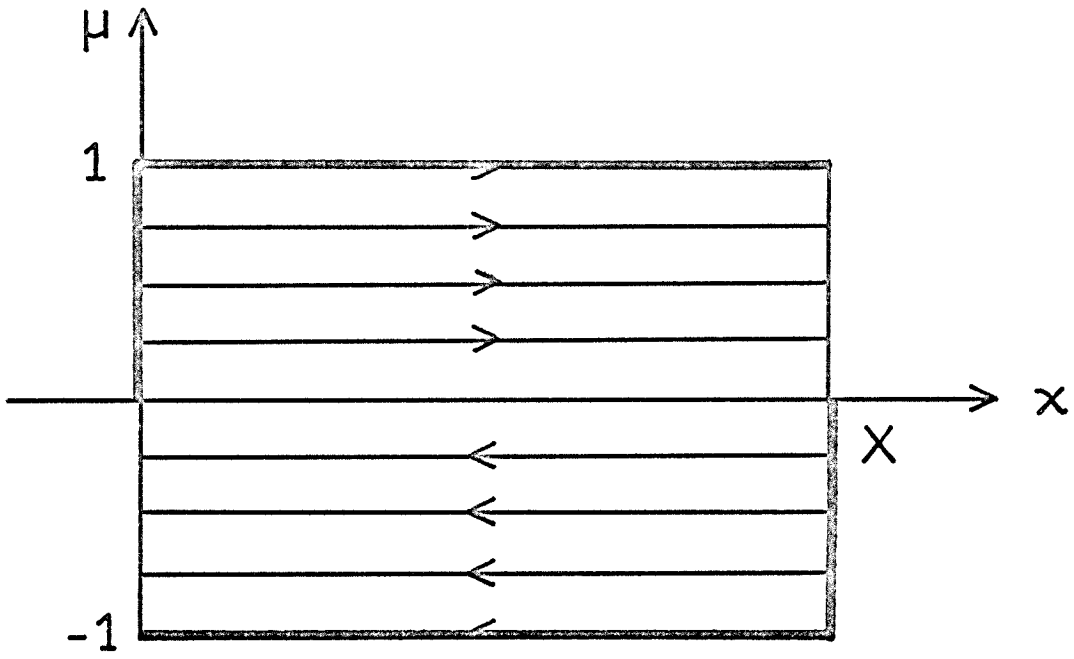

Figure 2. Phase Space

Figure 2 may be thought of as a box, into which particles may be injected. The solution is determined by specifying what particles are injected; the internal machinery of the box (the differential equation) determines what comes out. Taking account of the arrows, we see that the particles entering the box are described by $f(x = 0, \mu > 0)$ and $f(x = X, \mu < 0)$. These, then, are the data needed to specify a solution of (18): it is not an initial-value problem in x, but a two-point boundary-value problem. In the case of the solar wind, we must apply the condition that essentially no particles enter the system from interstellar space in order to determine the solution.

We must also apply boundary conditions at $\mu = \pm 1$, just as for the diffusion equation. Because of the spherical geometry, the equation is singular at $\mu = \pm 1$, and the condition that f be finite there is enough to determine it. In short, to determine the solution of our equation we must give boundary conditions on the part of the boundary that is heavily outlined in Figure 2.

Now, there is no known analytic solution of our problem, and we shall eventually solve it by numerical analysis. Numerical methods are extremely inefficient for two-point boundary-value problems; but fortunately, we can avoid this difficulty. The proton thermal speed in the solar wind near the earth is much less than the outward convection speed of $\simeq$ 300 km/sec. Therefore almost all the particles have very small pitch angles, and are concentrated near the top edge of Figure 2; hence, the number knocked down into the lower half-plane is

negligible, and the region $\mu < 0$ may be entirely disregarded. The problem now behaves like a simple parabolic equation, and may be solved as an initial value problem (in x). Now, even if the rate at which particles trickle down to the lower half of Figure 2 is small, yet if one waits long enough (i.e., goes to large enough x), a sizable fraction of the particles will have reached $\mu < 0$, and our method will fail. Our approximation is thus nonuniformly valid for large distances. Still, the region of validity certainly extends considerably beyond the earth, and so the method is good enough for us. If one is interested in the solution much farther out, one will have to take account of the boundary condition at infinity (or at the termination of the solar wind), and solve the full two-point boundary value problem.

Having laid out a strategy for the solution of (19), we must return to a point that was glossed over in its derivation. We assumed that the scattering is isotropic. If this is taken seriously, one finds that as the wind travels out from the sun, it is back-scattered; and if the wind extends very far out into interplanetary space, (18) predicts that it is practically all backscattered, and none gets out to the far reaches of the solar system. This is nonsense. The point is that isotropic scattering is likely only if the scattering centers are at rest. But in our case they are moving with the plasma — they <u>are</u> the plasma; hence (19) is valid in a frame in which the plasma is at rest. In general there may be no frame in which it is everywhere at rest; but the solar wind has practically constant speed in the region of interest, as is shown in §2.3, and therefore (18) is true in a frame traveling with that speed.

Analytic methods have produced no solution of (18); we might therefore consider solving it numerically. Second-order partial differential equations are tedious and expensive to integrate; and this equation has been derived under a number of very special assumptions. We prefer, therefore, to abandon it, and use a description of the plasma which may be more generally valid and useful.

The Equation of Bhatnagar, Gross, and Krook

The main properties of the Fokker-Planck equation are the following: (a) it conserves the mass, energy, and momentum of the plasma, (b) it describes relaxation to a Boltzmann distribution (in other words, it satisfies Boltzmann's H-theorem), (c) it is a second-order partial differential equation. The properties (a) and (b) must be satisfied by any reasonable model of collision processes; and they are the only vital properties. We have no great reason to believe that the deflections of particles in the solar wind are always small-angle and isotropic in the local rest frame; the Fokker-Planck equation is only one of many possible approximations to the true Boltzmann equation. We would like to find an equation which preserves the properties (a), (b), but is more easily solved.

A suitable equation has been proposed by Bhatnagar, Gross, and Krook (1954) (it is often called the BGK equation, and sometimes the Krooked equation). It has been used frequently in recent years to study various problems in gas dynamics in which the Navier-Stokes equations (or higher approximations of the same type) are inadequate.*

---

*See the various volumes of the Proceedings of the Symposia on Rarefied Gas Dynamics.

It may be described as the simplest form of Boltzmann's equation that satisfies the H-theorem and the conservation laws. The H-theorem says that if the distribution function is not Maxwellian, then it will change in such a way that it becomes Maxwellian; the conservation laws say that the density, momentum, and energy of the Maxwellian towards which it is tending at any time are the same as the density, momentum, and energy of the gas at that time. These conditions are satisfied by

$$\frac{Df}{Dt} = \nu (f_B - f) \tag{2-21}$$

where f_B is a Maxwell-Boltzmann distribution whose density, mean velocity, and temperature are the appropriate moments of f:

$$f_B = n (\pi \tau)^{-3/2} \exp\left[- (\underset{\sim}{v}-\underset{\sim}{u})^2/\tau \right], \tag{2-22}$$

where

$$\begin{aligned} n &= \int f(x,v)\, d^3v \\ \underset{\sim}{u} &= \frac{1}{n} \int \underset{\sim}{v}\, f\, d^3v \\ \tau &= \frac{2}{n} \int (\underset{\sim}{v}-\underset{\sim}{u})^2\, f\, d^3v \quad ; \end{aligned} \tag{2-23}$$

k is Boltzmann's constant, of course, and m is the particle mass; ν represents the collision frequency, and may be a function of v.

If the gas is nearly in equilibrium, then n, u, τ in (23) may be replaced by their equilibrium values, and (21) becomes a linear equation; in this form it has been extensively used for studies of sound propagation and other problems. In our case, however, the gas

is far from equilibrium, and the parameters are not varying slowly in any sense, so we must treat the full non-linear integrodifferential equation. From a mathematical point of view, its properties are not as clear as those of the Fokker-Planck equation; but its general behavior is the same: when it is solved forwards in x, the solution gets smoother and smoother, and therefore when it is solved backwards, even the smallest bump becomes more and more exaggerated, and the solution eventually diverges. The discussion of pp. 30-34 applies here, and accordingly, we shall solve (21) as an initial-value problem, understanding that it will give correct results in the region that we are interested in, even though it breaks down at large distances from the sun. The breakdown occurs when particles start to appear in the lower half of Figure 2, and this will be easily recognized in the solution if it should occur.

2.5 The Solution

We must first write down the BGK equation, in a form suitable for numerical solution. We saw in §2.3 that the motion of particles in the spiral interplanetary field is best described in terms of phase-space coordinates $r,U,V_\perp$, related to the ordinary velocities $u,v_\perp$ by (15), (16). Including the BGK collision term, the Boltzmann equation now becomes

$$\frac{\partial f}{\partial r} = \nu\,(f_B - f)\ . \qquad (2\text{-}24)$$

f_B is defined by (22), (23), and ν is now the effective number of collision per unit radial distanced traveled. ν may be a function of velocity, but since it depends upon the detailed physics of the scattering, we do not know what the function is. We shall therefore solve the equation with a constant ν, representing some kind of average value. We shall call ν the collision frequency, although it is actually the number of collisions per unit distance, not time.

(24) is a first-order ordinary differential equation in r, solved by the usual step-by-step methods. We begin with a Maxwell distribution, at some distance D from the sun. This is the point at which the transition from collision-dominated flow to the kinetic-theory regime takes place; all current models of the wind agree that $D \simeq .1$ A.U., as discussed in §2.2. We use dimensionless variables, normalized so that r = 1 at the starting point; then r = 10 at the earth if one takes D = .1 A.U. The bulk velocity is measured in units of the bulk velocity at r = D. The equation can be written in

dimensionless form, using these variables. If the bulk velocity is constant, then by shifting the origin in velocity space to the bulk velocity, we can get an equation in which the only dimensionless number is the collision frequency (in suitable units). The ratio of the bulk speed to the thermal speed does not appear in the equation, and therefore the solution does not depend upon it. This transformation is possible as long as the bulk velocity is constant, which is true if the thermal and gravitational energies are much less than the directed kinetic energy. This is in fact true in the solar wind beyond .1 A.U.; so it does not matter what value we choose for v_{th}/V_{bulk}, as long as it is small. For technical reasons (discussed in Appendix E), 1/100 is the largest value we can conveniently use. This corresponds to a temperature of $\sim 5.10^3$ ^oK at the earth, with a bulk speed of 350 km/sec. This is somewhat less than 3.10^4 ^oK, the average temperature of the Vela observations which we shall discuss below; but as long as we are interested in temperature ratios, not in predicting absolute temperatures, this does not matter (this may be seen in the formulae (12), (13) for the collisionless case, and remains true in the presence of collisions).

Finally, we must choose a value for the parameter R describing the spiral field (see (2)). We take R = 1 A.U., so that the spiral angle is 45^o at the earth. Our model is now fully determined, except for the value of the collision frequency ν, and we solve it for several different values of ν .

The differential equation (24) was solved by a second-order predictor-corrector method; ten steps between r = 1 and r = 10 gave

sufficient accuracy. At each step, the integrals (22) must be evaluated; this was done by Simpson's Rule, using a mesh of $\simeq 600$ points in the two-dimensional velocity space. More details of the numerical methods used will be found in Appendix E. It should be noticed that although the solution of partial differential equations is often imperiled by instabilities, we are safe from this danger. The main property of the BGK equation is that it damps out any local bumps in the distribution, and tries to make it as smooth as possible. Therefore any numerical errors will be damped out in the same way, and cannot lead to instability.

Results

Figure 3 shows the anisotropy factor $T_{\|}/T_{\perp}$ as a function of dimensionless distance, for various values of ν . If D = .1 A.U., then r = 10 at the earth; we determine ν by selecting the curve which gives the observed value of the anisotropy. The observed anisotropies of 1.5 - 4 require ν = .15 – .4; in other words, a typical particle makes, say, .25 collisions per unit radial distance traveled. Since we are using a distance unit of .1 A.U., this means that it makes 2.5 collisions between .1 A.U. and 1 A.U.

If one prefers a different value for the distance D at which the wind stops being collision-dominated, then instead of looking along the line r = 10 in Fig. 3, one looks along the line r = 1/D (where D is expressed in A.U.), and picks the value of ν that gives the observed anisotropy. The total number of collisions that a typical particle makes between D and 1 A.U. is then ν/D. (This is not quite

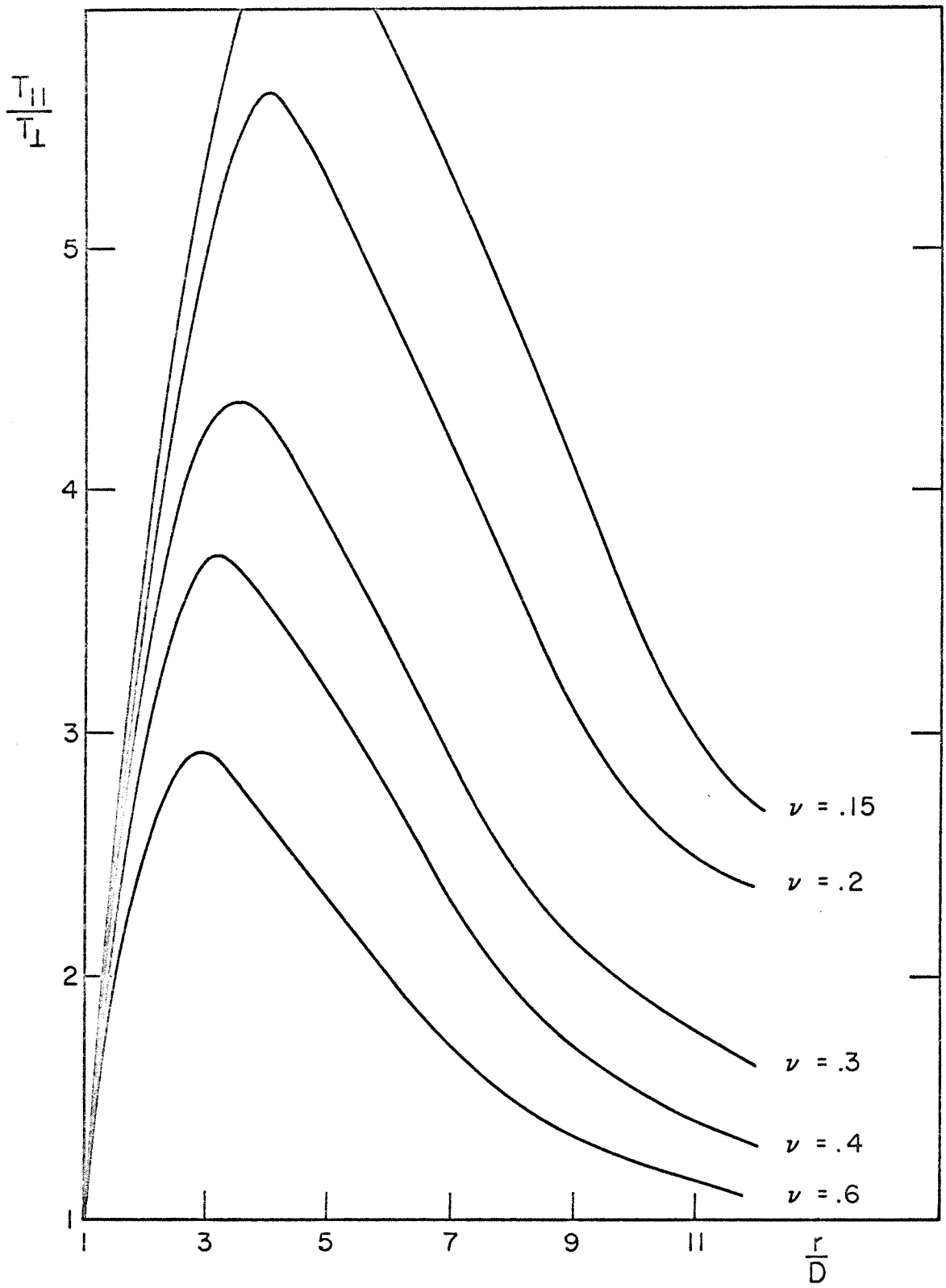

Figure 3. The anisotropy factor in the solar wind.

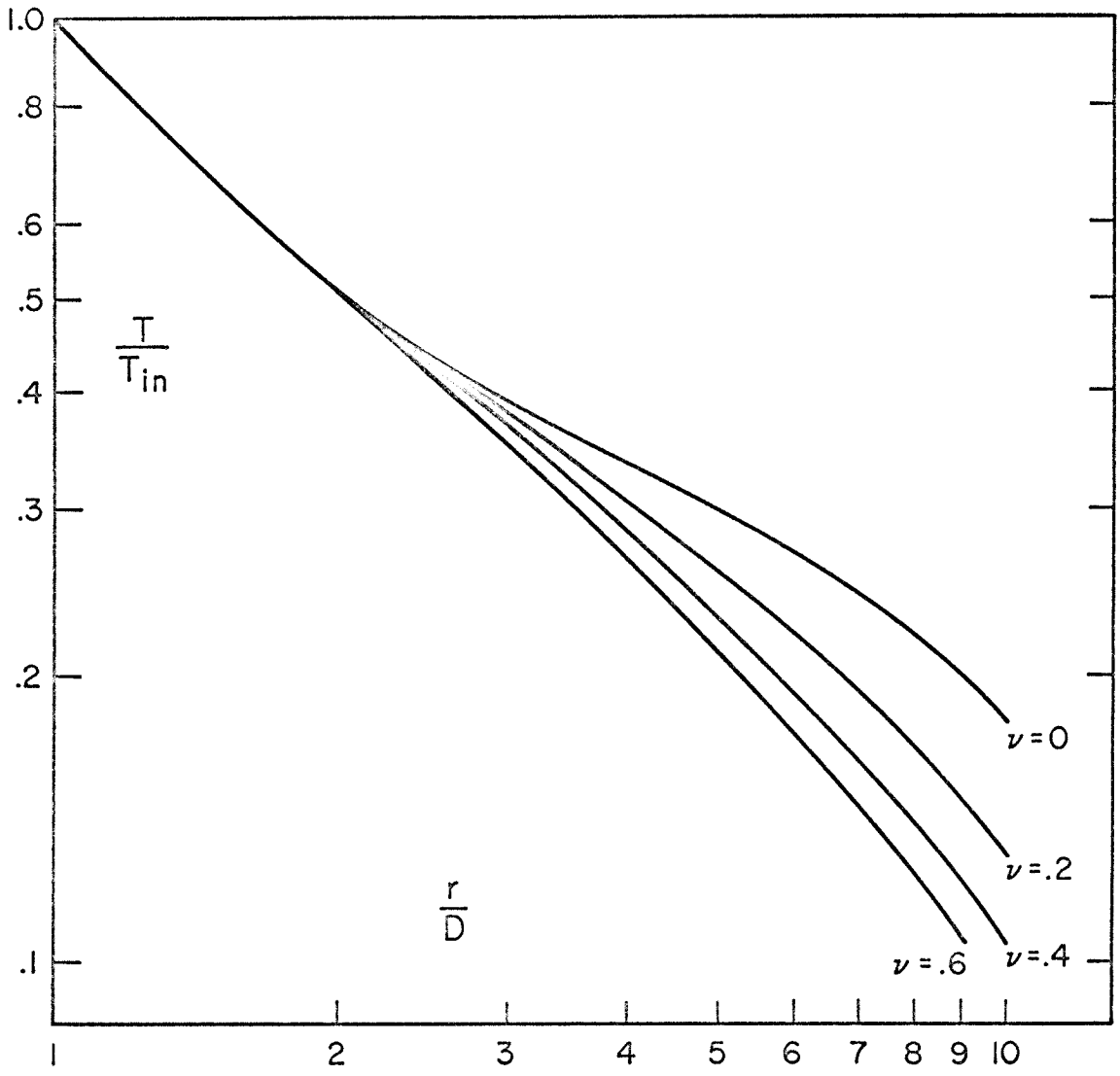

Figure 4. The mean temperature in the solar wind

correct: if D is changed, then the dimensionless value of R must be changed in order to keep the spiral angle 45^{o} at the earth. But as long as the change in D is small, the corresponding change in R has only a small effect on the solution, and may be neglected in first approximation).

Figure 4 is a logarithmic plot of the temperature T averaged over direction: $T = (T_{\parallel} + 2T_{\perp})/3$. On the whole it follows a polytropic law $T \propto n^{\gamma-1}$, with $\gamma = 1.5$. In other words, T is inversely proportional to distance from the sun. The deviation from this law is strongest when the collision frequency is zero. This is reasonable, for it is then that we expect the model to least resemble a polytropic gas. In general, the curves tend to become steeper at large distances, which means an increase in the adiabatic index γ. Parker (1963c) points out that at large distances, γ should rise to 5/3, the normal value for a gas with three degrees of freedom.

Figure 5 is a picture of the velocity distribution. We use coordinates with v_z along the magnetic field, and v_x perpendicular to it and in the ecliptic plane. The thermal velocities are symmetrical about the magnetic field; therefore the distribution has rotational symmetry about an axis in the v_z direction through the mean velocity (which is not in the z direction, because of the $\underset{\sim}{E} \times \underset{\sim}{B}$ drift). The figure shows f on the $v_z v_x$ plane (which contains the axis of symmetry), displayed by lines of equal f, drawn half an order of magnitude apart. It is drawn for the solar wind near the earth, with a collision rate of 2 collisions/A.U.

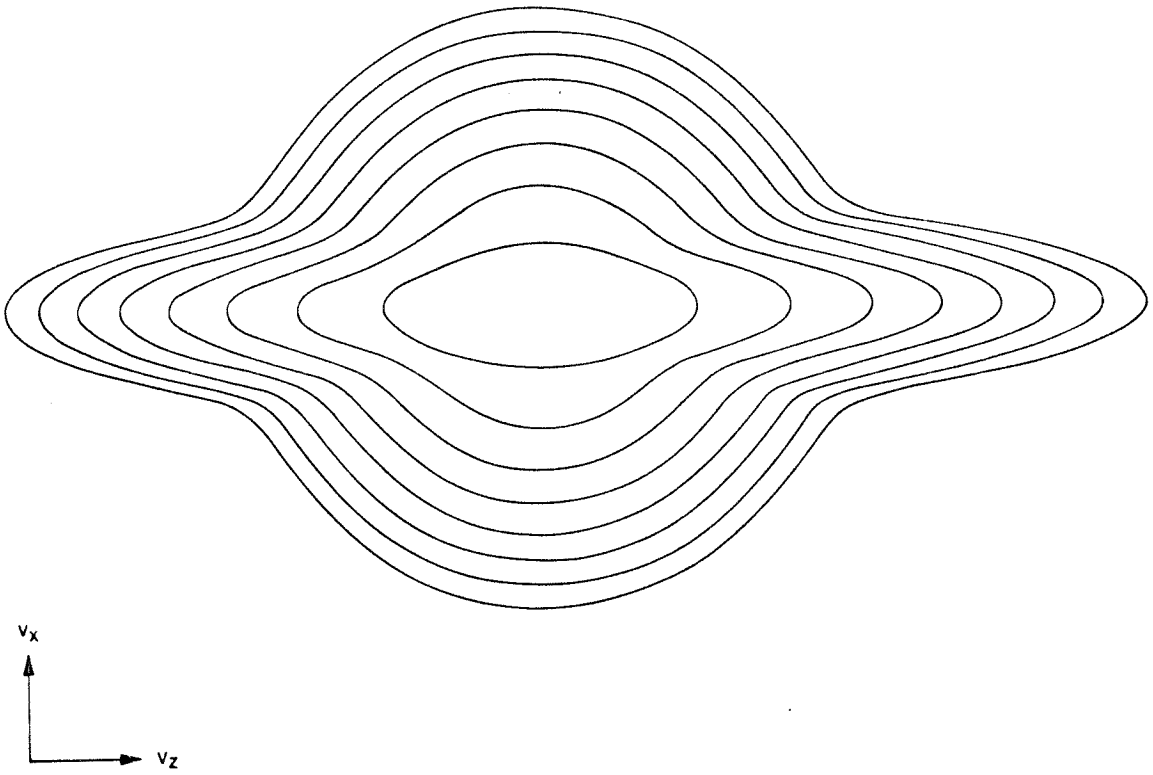

Figure 5. A contour map of the velocity distribution.

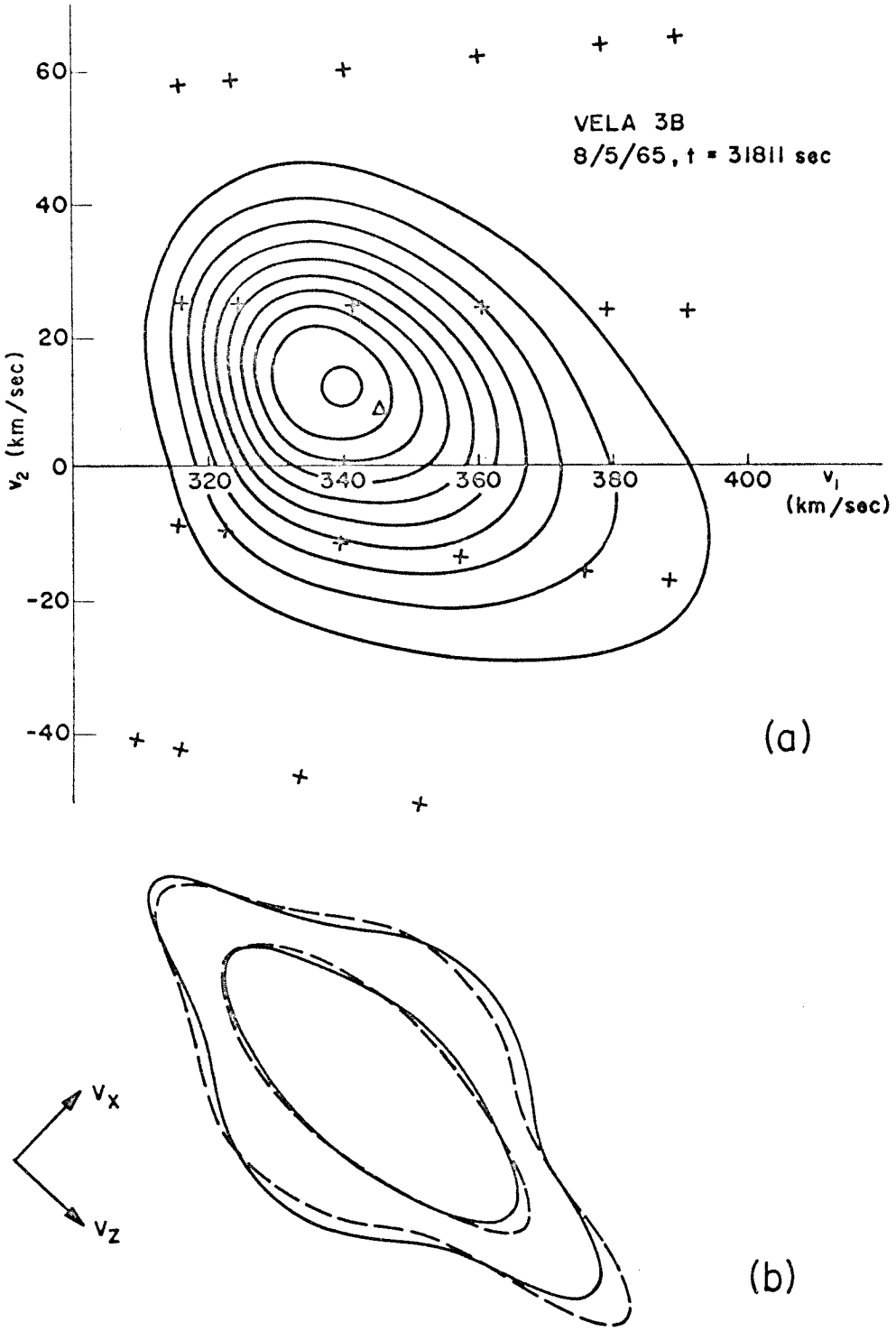

Figure 6. Velocity Distribution Functions

(a) Vela measurements

(b) Calculations: —— constant ν

- - - variable ν

Figure 6a is a contour map of the observed distribution function in the solar wind, as measured by the Vela 3 satellite (Hundhausen et al., 1967). The contours are drawn at intervals of 1/10 the maximum of f, so the area covered by all the contours in Figure 6a corresponds to the innermost two contours of Figure 5; they are redrawn in Figure 6b (the solid lines). The v_1 axis points away from the sun; the v_2 axis is less than 35^o away from the ecliptic, but its precise direction is not clear. When comparing Figures 6a and 6b, note that the crosses in Figure 6a represent points at which the distribution was measured; the contours are interpolated from those measurements.

The Vela data were taken during a fairly quiet period, when the mean temperature did not exceed 5.10^4 ^oK. At such times it is reasonable to treat the magnetic field as a spiral, plus some irregularities. On the other hand, at other times the temperature is often in the region of 5.10^5 ^oK. During these periods the plasma is presumably being heated by shocks and turbulence, caused by interacting high-velocity streams. The magnetic field, and indeed the whole situation, is much more complicated, and we need not expect our theory to apply to such periods of high temperature.

The outer parts of the computed distribution function of Figure 5 show definite horns lying along the direction of the magnetic field. The reason for this slightly peculiar shape is the following. The adiabatic cooling of the transverse temperature is much faster close to the sun, where the field is changing most rapidly; on the

other hand, we have assumed that the strength of the collision mechanism is independent of position. So when the plasma has traveled, say, .1 A.U. from its starting point, the field strength, and therefore $T_\perp$, has gone down by a factor of 4, while the collisions have not had enough time to seriously modify the distribution. Thus the plasma becomes very anisotropic early in its journey, and then later the collisions gradually drive it back towards isotropy (this can be seen in Figure 3). Now, when a non-equilibrium gas relaxes to a Maxwell distribution, the central part of the distribution relaxes faster than the outer parts; it takes much longer for collisions to affect the particles in the tail, and bring them to a Maxwell distribution. This seems plausible on general grounds; it has been observed by MacDonald, Rosenbluth and Chuck (1957) in numerical solutions of the Fokker-Planck equation. The evolution of the distribution may thus be described as follows. It begins as a spherical Maxwell distribution at .1 A.U.; it rapidly shrinks down to a cigar shape, as the magnetic field cools the transverse temperature; then gradually the collisions inflate the center of the cigar, and try to make it spherical, giving the state shown in Figure 5; and gradually the central sphere swells as it pulls in its horns.

This account depends on the assumption that the strength of the relaxation mechanism is more or less independent of distance from the sun. It is well-known that anisotropic plasmas tend to be unstable. One wonders whether the tendency of the plasma to develop extreme anisotropy near the beginning of its journey might trigger an instability,

producing a local concentration of waves at that point, which scatter the particles, and prevent the formation of the cigar-shaped distri-cution discussed above. For a plasma with $T_{\|} > T_{\perp}$, the dominant instability mechanism is the firehose instability. The criterion for its onset is

$$p_{\|} > p_{\perp} + \frac{B^2}{4\pi}$$

(Parker, 1958b, Longmire, 1963, p. 124). Near the earth, the magnetic and kinetic pressures are roughly equal,* so a pressure ratio of about 2 will be unstable. However, as we move towards the sun, the magnetic pressure increases faster than the mechanical pressure. According to our equation, if $\nu = .3$, the parameter $B^2/4\pi p_{\perp}$ at .2 A.U. is four times what it is at 1 A.U. So if the wind can support an anisotropy (i.e., pressure ratio) of 2 near the earth, it can support an anisotropy of 5 at .2 A.U. without triggering the firehose instability. The increased strength of the field stiffens the lines, and makes it harder to generate kinks in them.

There is another interesting feature of Figure 5: it is slightly asymmetrical. The distribution is spread out more in the direction away from the sun (large v_z) than towards it. This prediction is confirmed by the satellite observations, as is clear from Figure 6; the asymmetry is indeed rather stronger than our model suggests. One mechanism for producing it may be the following. The particles with

---

*As observed from Mariner 2 by Neugebauer and Snyder (1967).

greater v_z have traveled faster from .1 A.U., and have therefore spent less time on the journey, than those with smaller v_z. Now, the equation that we have solved assumed that the mean free path is independent of velocity, so that the number of collisions that a particle makes depends only on how far it travels, and not on how long it takes. However, this may not be so; it seems not unlikely that particles that take longer to reach the earth may therefore suffer more collisions. In this case they would be thermalized more rapidly: the low-velocity horn of the distribution (Fig. 5) will be drawn in and thermalized faster than the other, and the observed asymmetry will result.

To estimate the strength of this mechanism, a calculation was made with ν decreasing linearly with velocity; it was .2 at the peak of the distribution, and changed by .07 over one thermal speed. This is nearly twice as strong a variation as that expected if there is a constant number of collisions per unit time, even if the temperature is as high as 5.10^5 ^oK, with a bulk velocity of 350 km/sec. The broken curves of Figure 6b represent the results of this calculation. The degree of asymmetry is certainly no greater than that of Figure 6a, so it seems that such a strong v-dependence of ν is in fact needed to explain the data.

2.6 Discussion

In §2.2 we saw that the Boltzmann equation is always a correct equation, provided that the collision term is properly chosen. One wonders under what conditions the BGK equation is a good approximation. If one allows the collision frequency ν to be a function of position and velocity, there is a great deal of freedom in the BGK collision term. Indeed, it can be argued that there is <u>always</u> a $\nu(x,v,t)$ such that the BGK equation is satisfied. For any problem in kinetic theory, there is always a solution $f(x,v,t)$ — even though we may not be able to find it. If ν is defined by

$$\nu = \frac{Df/Dt}{f_B - f} \tag{2-25}$$

then the BGK equation is satisfied. The equation therefore is always correct if ν is properly chosen. If one desires infinite precision, it may be impossible to find the correct ν without using the formula (25), which is useless unless one already knows the solution f. But if one is interested mainly in the first few moments of f, then it is probably not too important to choose the correct velocity-dependence of ν .

If the dependence of ν on position is correct, then the BGK equation should give a complete description of the solar wind, in the inner as well as the outer regions. If ν is very large (as it is below .1 A.U.), then the BGK equation will reproduce the hydrodynamic results, and there is no point in using it. Its virtue is that it provides an accurate description of a gas, bridging completely the

range from collision-dominated to collisionless gases.

There is one important respect in which we have simplified the problem: we have been considering the motion of particles in a fixed magnetic field, and have not properly taken into account the effect of the particles upon the field. The magnetic field has been chosen to be consistent with a solar wind flowing radially outwards at constant speed V; since our solution very nearly does this, the magnetic field is consistent with the particle motions, to a very close approximation, and our results are in general accurate. However, certain details may be incorrect. In particular, the conservation of angular momentum has not been taken into account. This is the equation that relates the magnetic field to the azimuthal velocity, and allows us to determine a field consistent with the particle motions. If this conservation law is included in the system of equations, and the B field determined from it, then the BGK equation will give a complete description of the wind, including its angular momentum.

Now, our magnetic field differs only slightly from the true self-consistent field. From the angular momentum equation (see Weber and Davis, 1967) it follows that the (absolute) error in the azimuthal velocity is small. But the azimuthal velocity is itself small (compared with the total velocity); therefore even a small absolute error makes the results quite unreliable, and our calculation tells us nothing about the azimuthal velocity of the wind near the earth. It would be possible to solve the BGK equation including exact angular momentum conservation; this would predict the non-radial velocity. In the collision-dominated

region, it will presumably reproduce the results of Weber and Davis (1967), with much more labor, of course. In the outer region, one might expect some modification of their results; the predictions could be compared with the observations by Wolfe et al., (1966) of non-radial streaming in the solar wind. However, this is not a trivial modification of my calculation.

Another apparent deficiency of our model is that we have completely ignored the electrons, and treated the protons as if the only forces on them were the magnetic field, and collisions. The condition that this be valid is that there be no charge-separation, and therefore no electric field (apart from that required to make the magnetic field rotate with the sun). If we assume that this is true, then our equations are applicable to both the electron gas and the proton gas individually. In our model the particle density falls off as the inverse square distance from the sun, and is independent of the particle mass and charge. Therefore we will have equal densities for electrons and protons, which agrees with our assumption of no charge-separation fields. This assumption is thus consistent and correct.

Finally, we should discuss the theoretical status of the parameter ν. We have treated it as a phenomenological parameter, and determined an average value of $\simeq 2.5$ collisions/A.U. When more data become available on the anisotropy of the wind at different distances from the sun, we will be able to use the same method to determine the space-variation of ν — to solve the BGK equation with variable ν is as easy as with constant ν.

In principle, however, it is not necessary to treat ν as a phenomenological parameter. We believe that the 'collisions' are interactions of the particles with magnetic irregularities. If we knew the irregularities of the magnetic field in detail, we could work out the dynamics of the particle motion, and thus calculate the effective collision rate. In this way Jokipii (1966) has computed the diffusion coefficient for the scattering of cosmic rays in the solar wind, using measurements of the power spectrum of interplanetary magnetic fluctuations. We should be able to make a similar calculation of the diffusion coefficient of the solar wind particles themselves.

In order to produce scattering, a wave must be able to violate the adiabatic invariants of the particle motion — otherwise the magnetic moment is conserved, and the calculations of §2.3 apply. Therefore the wavelength must be at least as small as the gyroradius, $\sim$ 50 km. Since the wind is traveling at 300 km/sec. or more, such a wave will be swept past a spacecraft in 1/10th of a second at most, and therefore rather high resolution magnetometers and telemetry must be used. At present, there are no data on fluctuations at $\geq$ 10 c/s in the interplanetary field; but when they become available, we will be able to compute the parameter ν from first principles, and see how it compares with values deduced from measurements of the anisotropy.

III. INTERACTION WITH SOLID BODIES

3.1 Introduction

In Chapter 2 we considered the flow of the wind as it expands freely outwards from the sun. We shall now turn to the far more complicated question of what happens when it meets an obstacle in its path, such as a planet or satellite.

The most familiar example of such a problem is presented by the earth. The interaction here is dominated by the geomagnetic field. Magnetized plasmas from different sources tend not to mix: a sharp boundary is formed, at the point where the pressures balance, and the incident plasma is reflected from the boundary. Now, calculation of the shape and position of this interface is difficult, but the physics of its internal structure is reasonably well understood, at least in the limiting case appropriate to the interaction of the solar wind with the front of the magnetosphere (Rosenbluth, 1957). An individual-particle treatment suggests that particles are reflected specularly from the boundary, and cannot cross it. An exact treatment of the flow should include the structure of the boundary layer. But as long as it is thin, its detailed structure is unimportant, and the flow past the magnetosphere may be determined from some kind of fluid equation, with the boundary condition that the normal component of velocity vanish there. This situation is familiar in ordinary fluid mechanics; aerodynamicists have devoted much effort to the solution of flow around

blunt bodes with this boundary condition. One can use the intuition and experience gained in aerodynamics to reach a semi-quantitative understanding of the flow of the solar wind around the magnetosphere; and this has led, as is well known, to the successful prediction of the standing shock wave in front of the earth. The problem, then, is in outline reasonably well understood.

We shall be concerned here with the slightly more exotic problems posed by bodies which are not shielded by a magnetic field from contact with the solar wind. The comets have been the most studied of these — in fact, it was studies of comets which first showed the existence of a continuous solar wind. However, they present a very complicated problem. One of their unorthodox features is the continuous outflow of gas from the head of the comet; this has been treated by Biermann, Brosowski, and Schmidt (1967), using the hydrodynamical equations with source terms. Other processes which must be important are ionization of the cometary matter by the wind, and magnetic effects (see, for example, Beard, 1966). In view of the complexity of these problems, it seems a good idea to begin with the simplest problem in the class of non-magnetic bodies, and try to understand it on the same sort of level as we understand the interaction of the wind and the earth.

Accordingly, this chapter will be devoted to the study of solid bodies, with neither magnetic field nor atmosphere, moving through a plasma; we suppose the bodies much larger than the Debye length and the proton gyroradius ($\sim$10 m and 100 km, respectively, in the solar

wind). The moon very probably belongs to this class. It is very unlikely that a significant atmosphere has accumulated, since the solar wind is efficient in ionizing and sweeping away such gases as may seep to the surface. According to Explorer 35 (Sonett, Colburn, and Currie, 1967), the magnetic field between 700 and 7000 km. above the moon's surface is less than 2γ, which suggests that the moon does not have much magnetic moment. This view is supported by theoretical speculations, which generally agree that the earth's magnetic field is caused by motions in its fluid core (although no one has produced even an estimate of the geomagnetic field from this theory); the moon is so much smaller than the earth that its interior will be cooler, and may well be solid (though this is not at all certain). Furthermore, it rotates very slowly — once a month — and this makes significant dynamo effects in the interior very unlikely. It is therefore very plausible that the moon belongs to the class of problems we are considering.

The motion of Jupiter's satellites through its magnetosphere is another problem of the same type; it has raised a great deal of interest since Bigg's (1964) discovery that the radio emission from Jupiter is correlated with the orbital motion of the satellite Io. This correlation will presumably be understood once we fully understand the interaction of Io with the magnetospheric plasma through which it moves.

Mars is another possible candidate. The Mariner IV observations revealed no definite signs of a magnetosphere, or shock wave in the solar wind. If Mars has an intrinsic dipole field, it

should be surrounded by a magnetospheric configuration similar to that of the earth; the observations set an upper limit on the size of the magnetosphere, and applying the appropriate scaling laws, one finds that the surface field is less than 100γ, which is rather small.* So perhaps Mars has no dipole field. On the other hand, it certainly has an atmosphere, and the interaction of the wind with the atmosphere is a fairly complex matter, for which no satisfactory theory exists. Similar remarks apply to Venus.

We shall consider the simplest possible model of what happens when the solar plasma hits the surface of a planet (or satellite): we assume that any particle striking the surface is absorbed, and neutralized.** In §3.2 we shall study in detail the boundary layer at the edge of the plasma, and extract from this study the boundary conditions which must be imposed at the surface, in a fluid-mechanical treatment of the flow (the analog of the condition of reflection of particles from the magnetosheath). In §3.3 we shall apply this boundary condition to a two-dimensional model, of flow around a cylinder, and show that there is no steady solution of the fluid equations. This is very different from the magnetosphere problem, and shows that the boundary conditions in our case are somehow more stringent.

---

*Smith, Davis, Coleman, and Jones, 1965.

**We assume this as a basis for discussion, while recognizing that there are other possibilities.

3.2 The Transition Sheath

In this section we shall consider the boundary layer at the edge of a plasma in contact with a solid body; we are interested in the behavior of the density and magnetic field very close to the surface. We assume that whenever a particle hits the surface, it is absorbed, and neutralized (as long as the body is large compared to the Larmor radius, roughly equal numbers of electrons and protons hit it, so neutrality is not unreasonable).

We do not expect electrostatic forces to play a dominant rôle in the structure of the sheath. In the theory of the transition layer between a plasma and a magnetic field (Rosenbluth, 1957), it is found that if one works with an imaginary plasma composed of equal-mass particles, one reaches results very similar to the exact solution of the unequal-mass problem, as long as the mass of the particles in the model is chosen to be some appropriate combination of the electron and proton masses — in this case, the geometric mean. We expect that our problem behaves in the same way, and we shall accordingly work with an equal-mass plasma.

Since we are considering planets much larger than a gyroradius, and planets do not have sharp edges, we can ignore the curvature of the boundary, and set up a one-dimensional problem. As a final simplification, we shall at first suppose that the plasma is at rest relative to the body.

Our aim is to find the magnetic field as a function of

distance from the wall. The method is to first consider an arbitrary $\underset{\sim}{B}$ field; compute the motions of the particles in that field; compute the current produced by those motions; and finally, determine $\underset{\sim}{B}$ by requiring those currents to be consistent with the magnetic field that we started with — that is, by applying Ampères law. Owing to the high symmetry of our problem, and to the absence of electric fields, we shall be able to find an exact self — consistent solution, without any dubious approximations. It would clearly be wrong, for example, to use the adiabatic approximation for the particle orbits, since we expect that in the transition layer, the field may change rapidly over a gyroradius.

The Orbits

We consider a one-dimensional problem, with a magnetic field $\underset{\sim}{B}(x)\ \underset{\sim}{\hat{z}}$ ($\hat{}$ denotes a unit vector) filling $x \leqslant 0$, and an absorbing surface at $x = 0$. In a given field, the orbit of a particle is determined by its initial position and velocity. Through every point of the half-space $x < 0$, there pass an infinite number of possible trajectories, pointing in all directions. In an undisturbed equilibrium plasma, the particles will be uniformly distributed over these possible orbits, the flux will be isotropic, and there will therefore be no net current.

Close to an absorbing wall, however, things are different. Some of the orbits will intersect the wall; there can be no particles traversing these orbits. At points close to the wall, therefore, not all directions of motion are available to the particles: there are forbidden regions in velocity space. By doing some geometry on the

orbits, we can find these forbidden regions.

The equations of motion of a particle with charge $\pm e$ ($e > 0$) are

$$\ddot{x} = \pm \omega \dot{y} \quad ,$$

$$\ddot{y} = \mp \omega \dot{x} \quad ,$$

where

$$\omega = \frac{e}{mc} B(x) \quad .$$

The z equation says that the particles travel with constant speed along the lines of force; this motion is irrelevant to our calculations.

We define

$$\psi(x) \equiv \int_0^x \omega(x')\, dx' \; ; \tag{3-1}$$

it is the y-component of the vector potential. We may now rewrite the equations of motion, using $d/dt = v_x d/dx$:

$$v_x v_x' = \pm \psi' v_y, \tag{3-2}$$

$$v_x v_y' = \mp \psi' v_x, \tag{3-3}$$

where ' stands for d/dx. (3) is immediately solved:

$$v_y = \kappa \mp \psi(x) \; , \tag{3-4}$$

and so,

$$v_x = \sqrt{v^2 - (\kappa \mp \psi)^2} \; , \tag{3-5}$$

by energy conservation. κ and v are constants of integration: each

orbit is labeled by definite values of κ and v, and (4) and (5) then describe the orbit. v, of course, is the absolute velocity of the particle, which is constant in a magnetic field.

Let $\xi(\kappa,v)$ be the greatest value of x achieved by the orbit labeled (κ,v). Then $\xi(\kappa,v) > 0$ is obviously the condition for the orbit (κ,v) to intersect the wall, that is, for it to be a forbidden orbit.

Now, since ξ is the maximum x,

$$v_x \ (x = \xi) = 0 \ .$$

From (5), therefore,

$$(\psi(\xi) \mp \kappa)^2 = v^2 \quad . \tag{3-6}$$

ξ is, by definition, the larger of the two roots of this equation.

We shall restrict ourselves now to magnetic fields which always have the same sign — it is wildly unlikely that the self-consistent solution will have a reversal of the field. ω is therefore positive, and by (1), ψ is a monotonic increasing function. Therefore the larger root, ξ, of (6) corresponds to the larger value of $\psi(\xi)$, which is

$$\psi(\xi) = + v \pm \kappa \ . \tag{3-7}$$

This equation determines $\xi(\kappa,v)$, if ψ is a known function.

Now, for allowed orbits, $\xi < 0$, as we have seen; and $\psi(0) = 0$ (see (1)); so

$$\psi(\xi) < 0 \ ,$$

or

$$v \pm \kappa < 0 \ , \tag{3-8}$$

for allowed orbits.

This result is not in a very useful form; κ is a parameter characterizing the orbit, but its physical interpretation is not clear.

If θ is the angle between the x axis and the velocity vector of a particle, at the point x, on the orbit labeled (κ,v),

$$\sin\theta = \frac{v_y}{v} = \frac{\kappa \mp \psi(x)}{v} \ , \tag{3-9}$$

by (4). For each x and v, some direction will be allowed, some forbidden. The allowed directions satisfy (8), which, in terms of θ, becomes

$$\sin\theta \lessgtr \mp\left[\frac{v + \psi(\xi)}{v}\right]$$

(upper signs for + particles, lower for -).

Define Θ by

$$\sin\Theta = 1 + \frac{\psi(\xi)}{v} \ , \ -\frac{\pi}{2} < \Theta \leqslant \frac{\pi}{2} \ . \tag{3-10}$$

Then

$$\sin\theta \lessgtr \sin \mp\Theta$$

or

$$\Theta - \pi < \theta < -\Theta \quad \text{for + particles,} \tag{3-11}$$

$$\Theta < \theta < \pi - \Theta \quad \text{for - particles .} \tag{3-12}$$

(11) and (12), with (10) define the allowed regions in velocity space.

The Current

In order to completely specify our problem, we must give the distribution function in the allowed regions. We shall set up the problem by supposing that in the distant past there was a completely uniform plasma, with no boundaries. An absorbing wall was then introduced, at x = 0, and the system allowed to readjust itself, and come to a new equilibrium, the object of our present study. Now, according to Liouville's Theorem, the distribution function is constant along particle trajectories. Therefore, at each point in the allowed region of phase space for the final state, the distribution function is equal to the value at the corresponding point of phase space for the initial state; and we have assumed this to be independent of x and θ (where θ is the direction of the velocity — cf. (9)). Thus $f(x,v,\theta)$ is independent of x and θ in the allowed regions, and vanishes elsewhere:

$$f^{+} = \begin{cases} \frac{N}{2\pi}\, g(v) & \text{if } \Theta - \pi < \theta < -\Theta \\ 0 & \text{otherwise,} \end{cases}$$

and

$$f^{-} = \begin{cases} \frac{N}{2\pi}\, g(v) & \text{if } \Theta < \theta < \pi - \Theta \\ 0 & \text{otherwise,} \end{cases}$$

are the distribution functions for ± particles respectively; N is the density in the initial state, Θ is defined by (10), and g(v), the distribution of speeds, may be chosen any way we wish.*

---

*It should be noticed that it was not absolutely necessary to go through the above verbiage in order to justify this distribution function. We are looking for a self-consistent solution, and can make any kind of assumption that we please about the solution, provided that it is justified in the end by the demonstration that it does indeed satisfy the equations.

We can now compute the current density at each point in the plasma:

$$j_y(x) = e \int d^2v \; v \sin\theta \left[f^+ - f^- \right]$$

or

$$j_y(x) = -\frac{2}{\pi} Ne \int_0^\infty v^2 \, dv \, g(v) \left[1 - \left(1 + \frac{\psi(x)}{v} \right)^2 \right]^{\frac{1}{2}}, \quad (3\text{-}13)$$

using (10).

To make further progress, we must specify g(v). We shall assume, for the present, that all particles have the same speed U, so that

$$g(v) = \frac{1}{U} \delta(v-U)$$

and therefore

$$j_y(x) = -\frac{2}{\pi} N \, eU \sqrt{1 - \left(1 + \frac{\psi(x)}{U} \right)^2} \quad . \quad (3\text{-}14)$$

This is an expression for the current, if the radical is real. If x is such that $[1 - (1 + \psi/U)^2]$ is negative, then there is no real Θ satisfying (10), so no forbidden regions; at such points the particle flux is isotropic and there is no current. So (14) should be supplemented by

$$j_y(x) = 0 \text{ if } \left(1 + \frac{\psi(x)}{U} \right)^2 > 1 \quad . \quad (3\text{-}15)$$

The Solution

Ampère's law reads

$$\frac{dB}{dx} = -\frac{4\pi}{c} j_y$$

or

$$\frac{d^2\psi}{dx^2} = \frac{8Ne^2U}{mc^2}\sqrt{1 - \left(\frac{\psi}{U} + 1\right)^2} \quad . \tag{3-16}$$

This differential equation determines the self-consistent solution for the vector potential. In dimensionless variables

$$a \equiv \frac{\psi}{U}, \quad X \equiv x\sqrt{\frac{8Ne^2}{mc^2}} \tag{3-17}$$

it becomes

$$\frac{d^2a}{dx^2} = \sqrt{1 - (1 + a)^2} \tag{3-18}$$

$$= 0 \text{ if } (1 + a)^2 > 1 \quad .$$

This type of equation may be thought of as the equation of motion of a fictitious particle in a potential field. Indeed, (18) has a first integral:

$$\frac{1}{2}\left(\frac{da}{dX}\right)^2 + V(a) = \text{const.}, \tag{3-19}$$

where

$$V(a) = -\int da\sqrt{1 - (1 + a)^2} \quad . \tag{3-20}$$

This is the energy equation for a particle in a potential field V(a), or, alternatively, for a particle in a uniform gravitational field sliding along a curve whose equation is z = V(a). a(X) in our problem corresponds to x(t) for the fictitious particle, and a'(X), which is proportional to the magnetic field, corresponds to v(t) for the fictitious particle.

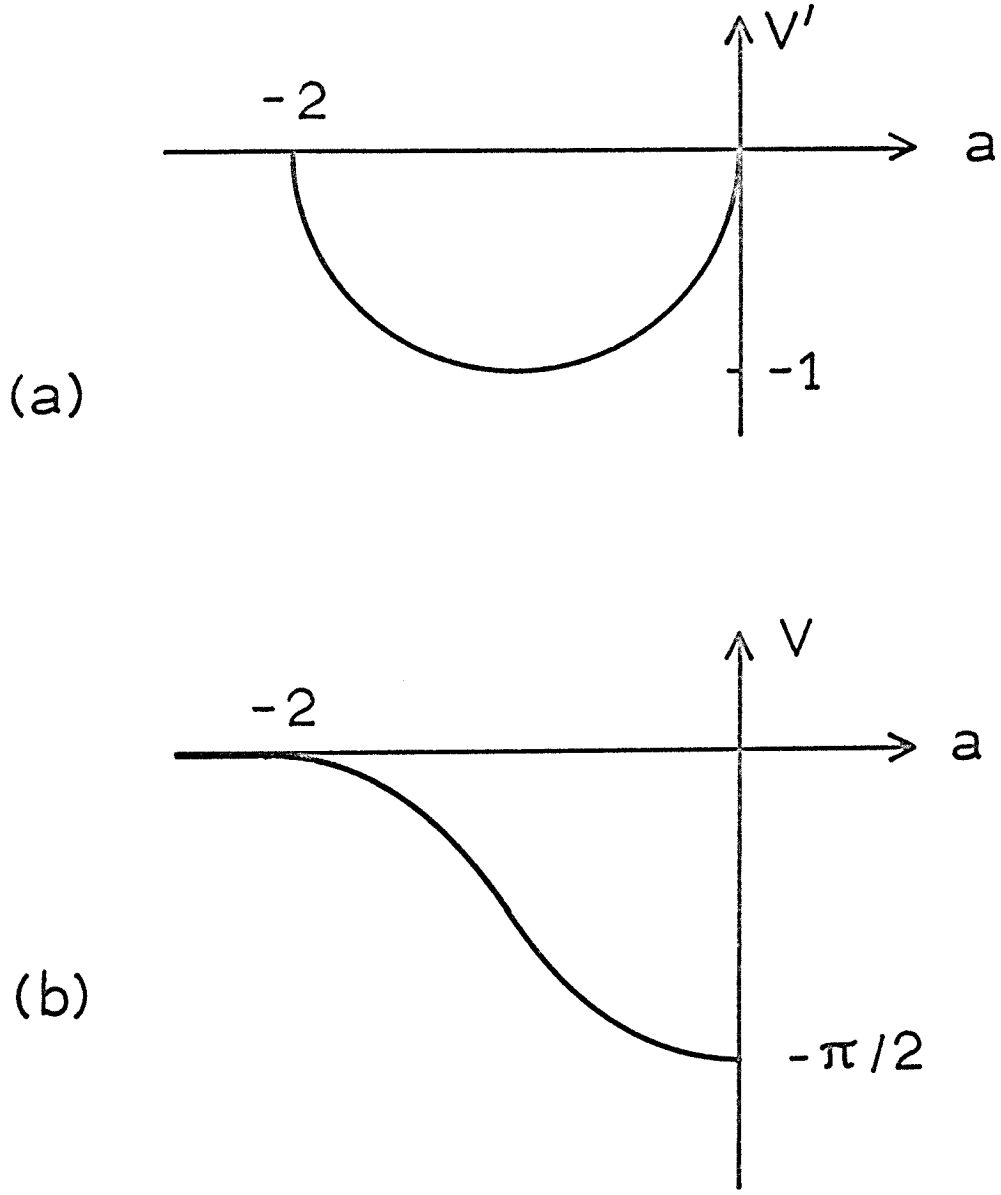

Figure 7.

(a) The force on the fictitious particle

(b) The potential

Figure 7a shows V' as a function af a, and in Figure 7b is sketched V itself. A particle sliding to the right along this curve has constant speed until it reaches a =-2, and then it speeds up as it approaches the wall. So, in our problem, B is constant beyond a certain distance from the wall, and increases close to the wall. In fact, from (19),

$$\frac{B_o^2}{8\pi} - \frac{B_\infty^2}{8\pi} = NmU^2 \qquad (3\text{-}21)$$

This is the pressure balance equation: B increases just enough to balance the loss in kinetic pressure as the density falls to zero at the surface. This is the boundary condition that we need: given the pressure and field at the outer edge of the sheath, we can use it to calculate the field at the inner edge, that is, at the surface of the solid body. For the purpose of studying the windflow around planets, we do not need to know anything else about the structure of the layer, as long as we know the change in B across it, and as long as it is thin (compared to the radius of the planet).

The Thickness

Since we have derived a dimensionless equation for the structure of the sheath by writing

$$X = x\sqrt{\frac{8Ne^2}{mc^2}},$$

one might be tempted to suppose that its thickness is of the order

of $\sqrt{mc^2/8Ne^2}$. However, this would be rash: there is a dimensionless number concealed in our problem, namely, the ratio of dynamical to magnetic transverse pressure* in the undisturbed plasma, usually called beta:

$$\beta = \frac{8\pi NmU^2}{B_\infty^2} = \left(\frac{\text{gyrospeed}}{\text{Alfven speed}}\right)_\infty^2 .$$

Now,

$$\frac{da}{dX} = \frac{B(X)}{B_\infty}\sqrt{\frac{\pi}{\beta}} \to \sqrt{\frac{\pi}{\beta}} \qquad \text{for large } (-X) .$$

So the terms in (18) are not necessarily of order 1, and we must be careful in evaluating the scale length of the sheath.

From (19), we have

$$\left(\frac{da}{dX}\right)^2 + 2\,V(a) = \left(\frac{da}{dX}\right)_\infty^2 = \frac{\pi}{\beta} ,$$

so

$$\frac{da}{dX} = \sqrt{\frac{\pi}{\beta} - 2V(a)} .$$

Now, a runs from -2 at one edge of the sheath to 0 at the other (see Fig. 7). Therefore the total thickness of the sheath is given by

$$\Delta X = \int_{-2}^{0} \frac{da}{\sqrt{\frac{\pi}{\beta} - V(a)}} .$$

---

*It is only the pressure perpendicular to the field that is of interest here; the particles may have arbitrary velocities along the field without affecting our calculations.

We shall make a crude estimate of this integral, by approximating the curve V(a) (Fig. 7b) by a straight line; this should be accurate to within factors of $\pi/2$ and the like. The result is

$$\Delta X \sim 2\left(\frac{\sqrt{1-\beta}-1}{\sqrt{\beta}}\right)$$

$$\sim \sqrt{\beta} \qquad \text{for small } \beta$$

$$\sim 2 \qquad \text{for large } \beta \ .$$

In dimensional variables, then, the thickness of the layer is

$$\sqrt{\frac{mc^2}{2Ne^2}} \left(\frac{\sqrt{1+\beta}-1}{\sqrt{\beta}}\right)$$

or

$$\Delta = R\sqrt{4\pi}\left(\frac{\sqrt{1+\beta}-1}{\sqrt{\beta}}\right)$$

where R is the free-stream gyroradius.

For small β, $\Delta \sim 2R$, which is the result one expects. But in a high-β plasma (magnetic pressure weak compared to kinetic pressure) the thickness is reduced by a factor $\sqrt{\beta}$.

In the solar wind, β is small, and the sheath is therefore a couple of gyroradii thick, so $<$ 200 km, say. As was discussed earlier, R is to be interpreted as some combination of the electron and proton gyroradii. Precisely what combination it is cannot be decided without solving the problem with unequal masses, and this presents some mathematical complications.

Generalizations

Our calculations were made for a plasma in which all the particles have the same energy. If this is not so, then the right hand side of (18) and (16), which is essentially the current (13), is a superposition of functions of the same form, but with different values of U. This means that the curves of Figure 7 are somewhat smeared out, but their general shape remains the same — except that the potential goes asymptotically to zero at large distances, instead of vanishing at some finite point. So the general character of the solution is unchanged. The change in B across the sheath will be given by the pressure balance equation, as before.

It is trivial to extend the theory to cases where the plasma is moving parallel to the wall: working in the rest frame of the plasma reduces this to the case we have considered above. It is far from trivial, however, to study the problem when the plasma is moving towards the wall.

We have mentioned that the jump condition across the sheath is what is expected from considerations of pressure balance. This statement may be made more precise by computing the pressure tensor for our distribution function. One then finds that

$$\frac{B^2}{8\pi} + P_{xx} = \text{const.}, \qquad (3\text{-}22)$$

where P_{ij} is the pressure tensor, and x is normal to the surface. This result might have been expected on general grounds; having

reached it from first principles in the case where the magnetic field is parallel to the surface, we may reasonably expect it to be true when the field is inclined to the surface. However, we must then restrict ourselves to the case where the particles have no velocity along the field.

The normal component of $\underset{\sim}{B}$ will be constant in the sheath, since div $\underset{\sim}{B} = 0$; the parallel component will increase by $\sqrt{8\pi\ P_{xx}}$. The field will therefore look like Figure 8 . Now,

$$P_{xx} = \rho \langle v_x v_x \rangle ,$$

where ρ is the mass density and $\langle\ \rangle$ denotes the average. We suppose that the particles in the undisturbed region are gyrating with speed U around field lines at angle θ to the surface. In a coordinate system aligned with the field lines, the tensor $\langle v_i v_j \rangle$ is

$$\frac{U^2}{2} \begin{pmatrix} 0 & & \\ & 1 & \\ & & 1 \end{pmatrix}.$$

Rotating through θ back to the xyz axes, we find

$$P_{xx} = \tfrac{1}{2} \rho\ U^2\ \cos^2\theta$$

in the undisturbed region; and $P_{xx} = 0$ at the surface of the wall; so

$$\frac{B_o^2}{8\pi} - \frac{B_\infty^2}{8\pi} = \tfrac{1}{2} \rho\ U^2\ \cos^2\theta \quad . \tag{3-23}$$

This agrees with (21) when $\theta = 0$ (note that $\rho = 2mN$, counting both

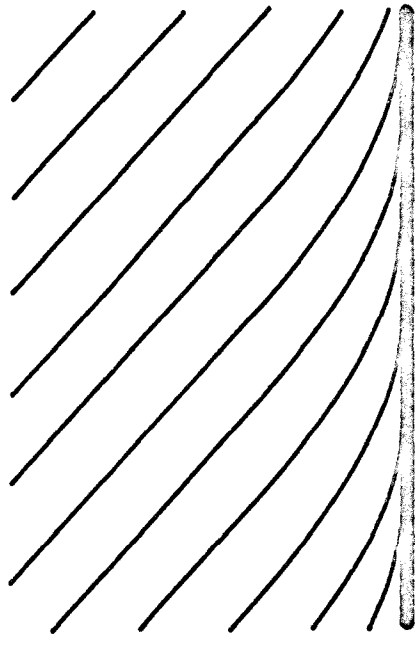

Figure 8. Magnetic field at the surface, with inclined geometry.

+ and - particles). When $\theta = \pi/2$ (field normal to the wall), it gives $B_o = B_\infty$, which is also correct. For in this case the particles are gyrating in planes parallel to the wall, and therefore never intersect it; the wall has no effect on the plasma at all. (23) is thus a reasonable jump condition for the sheath.

When $\theta = 0$ or $\pi/2$, the field lines are straight; the motion along the field is trivial, and does not affect our theory. But when the field is inclined to the surface, as in Figure 8, motion along the field carries a particle into regions of varying $\underset{\sim}{B}$, and complicates the dynamics considerably. For $0 < \theta < \pi/2$, then, (23) is true only when the particles have no motion along $\underset{\sim}{B}$. To treat a more realistic case will take further detailed study. For the rest of this chapter, however, we shall need only the case $\theta = 0$.

3.3 Application to Two-dimensional Flow

In §3.2 we have derived the boundary condition which must be applied to the plasma equations at the surface of a solid body. We shall now apply it to the flow around planets. This is a mathematically complicated problem; it seems reasonable to approach it by considering a two-dimensional model — this strategy produces useful results for the flow around the earth's magnetosphere. We propose to consider the flow of plasma around an infinite circular cylinder, with the magnetic field in the plasma parallel to the axis of the cylinder. The cylinder is supposed to have finite and uniform conductivity σ. One attraction of this model is that the magnetic and kinetic pressures are both isotropic (in the xy plane perpendicular to the axis).

There are three regions in space to be considered: the interior of the cylinder, the transition sheath, and the plasma outside. We shall treat the plasma as a perfectly conducting fluid. This is a satisfactory approximation everywhere except close to the body, and there we have an exact kinetic — theory treatment of the boundary layer.* All that we need to know about the sheath is: it is thin; the change in $B^2/8\pi$ across it equals the dynamical pressure; and the tangential electric field is continuous across the sheath, since curl $\underset{\sim}{E}$ is finite (zero in a steady state).

Theorem I

In a steady state, the flow is always tangential to the cylinder.

For, since curl $\underset{\sim}{E} = 0$ in a steady state,

$$\oint \underset{\sim}{E} \cdot \underset{\sim}{ds} = 0$$

integrated around any closed contour. We shall choose a contour surrounding the cylinder, and lying entirely in the hydrodynamical region, outside the boundary layer. Then $c\underset{\sim}{E} = \underset{\sim}{v} \times \underset{\sim}{B}$, and we have

$$\oint \underset{\sim}{v} \times \underset{\sim}{B} \cdot \underset{\sim}{ds} = 0 ,$$

or

$$\oint v_{\perp} B ds = 0 , \qquad (3\text{-}24)$$

---

*Just as, if the Reynolds number is large, inviscid fluid dynamics is a good approximation to the Navier-Stokes equations everywhere except in the boundary layer, where the full equations must be solved.

where $v_\perp$ is the component of $\underset{\sim}{v}$ perpendicular to the contour.

If we apply this to a circle, surrounding the cylinder, just on the outside edge of the sheath, then $v_\perp$ is the velocity perpendicular to the cylinder at its surface. Since plasma is never ejected from the cylinder, $v_\perp$ is never negative. In such a two-dimensional problem with straight B lines, the field can never be reversed; so B is always positive. The integrand in (24) is thus never negative, and therefore (24) demands that it vanish; since B is always positive, this proves the theorem.

We shall now use it to prove the following:

Theorem II

There is no steady solution to the problem of two-dimensional compressible ideal ($\sigma = \infty$) MHD flow around a (finitely) conducting cylinder, with magnetic field uniform at infinity, and parallel to the axis of the cylinder, and using the boundary condition of §3.2.

To deal with a flow problem such as this, we must consider the fields both inside the body and in the hydrodynamic region, and couple them by the appropriate boundary conditions. We shall first consider the interior fields. We assume, for simplicity, that the cylinder is of uniform conductivity; similar but more complicated results may be expected for other cases. The solution of the external flow problem will provide us with values of the electromagnetic field at the surface of the cylinder. We must then solve the time — independent Maxwell equations in its interior, with those values as boundary values. This raises the question: given the fields on a closed surface, does

there always exist a solution in the interior? The answer is no, in both the two-dimensional and the three-dimensional cases. Roughly speaking, Maxwell's equations, without Ohm's law, suffice to determine the interior fields from the boundary values. Ohm's law is then an extra constraint, which can be satisfield only if the boundary values fulfill certain conditions. These are worked out in Appendix B, for both two-dimensional and three-dimensional cases; the result that we need here is

$$B(\theta) = b + \frac{\sigma}{4\pi^2} \oint d\varphi \, E_\theta(\varphi) \log \left| 2 \sin \left(\frac{\varphi-\theta}{2}\right) \right| \qquad (3\text{-}25)$$

where $B(\theta)$, $E_\theta(\theta)$ are the magnetic and tangential electric fields at the surface, and b is an arbitrary constant. This condition on the surface is the only constraint that the interior Maxwell equations impose upon the external fields.

Now, according to Theorem I, $v_\perp = 0$ at the outer edge of the transition sheath. Therefore $E_\parallel = 0$ there. Since $E_\parallel$ is continuous across the sheath, $E_\parallel = 0$ on the surface of the cylinder. Now (25) says that B is constant on the surface, = b. Therefore at the inner edge, r = 1, of the hydrodynamical region, the jump condition (21) gives

$$B(1,\theta) = \sqrt{b^2 - 8\pi p(1,\theta)}\,, \qquad (3\text{-}26)$$

where $p(r,\theta)$ is the pressure. This, together with $v_\perp = 0$, is the boundary condition to be applied at r = 1 to the fluid equations, which we shall now discuss.

The standard hydromagnetic equations are too well-known to need much discussion. For our steady two-dimensional problem, they are

$$\rho(\underset{\sim}{v}\cdot\underset{\sim}{\nabla})\underset{\sim}{v} + \underset{\sim}{\nabla}\left(p + \frac{B^2}{8\pi}\right) = 0, \tag{3-27}$$

$$\underset{\sim}{\nabla}\cdot(\rho\ \underset{\sim}{v}) = 0\ , \tag{3-28}$$

$$c\underset{\sim}{E} + \underset{\sim}{v} \times \underset{\sim}{B} = 0, \qquad \underset{\sim}{\nabla} \times \underset{\sim}{E} = 0\ , \tag{3-29}$$

$$\underset{\sim}{\nabla} \times \underset{\sim}{B} = \frac{4\pi}{c}\ \underset{\sim}{j}, \qquad \underset{\sim}{\nabla}\cdot\underset{\sim}{B} = 0\ , \tag{3-30}$$

where ρ is the mass density.

The electromagnetic equations (29) combine to give

$$\underset{\sim}{\nabla} \times (\underset{\sim}{v} \times \underset{\sim}{B}) = 0\ ,$$

and this, in conjunction with the continuity equation (28), yields

$$(\underset{\sim}{v}\cdot\underset{\sim}{\nabla})\ \log\ (B/\rho) = 0.$$

Hence B/ρ is constant along streamlines, and since conditions are uniform far upstream, the constant has the same value on all streamlines. Therefore

$$\beta \equiv \frac{B}{\rho} \tag{3-31}$$

is a constant everywhere. We can use this relation to eliminate B from Euler's equation (27).

Now we must choose an equation of state for the plasma. For two-dimensional problems, with no gradients along field lines, it may be proved (see, e.g., Longmire, 1963), within the limitations of the

adiabatic approximation to the particle orbits (which is applicable to our problem outside the boundary layer), that

$$p = \kappa\rho^{\gamma} ,$$

with $\gamma = 2$ (this is the Chew-Goldberger-Low result).

We can now eliminate both p and B from Euler's equation (27), which becomes

$$\tfrac{1}{2}\,\underset{\sim}{\nabla}\, v^2 - \underset{\sim}{v} \times (\underset{\sim}{\nabla} \times \underset{\sim}{v}) + \underset{\sim}{\nabla}\left[\frac{\kappa\gamma}{\gamma-1}\,\rho^{\gamma-1} + \frac{\beta^2}{8\pi}\,\rho\right] = 0 .$$

Dotting with $\underset{\sim}{v}$, we have

$$\underset{\sim}{v}\cdot\underset{\sim}{\nabla}\left[\frac{v^2}{2} + \frac{\kappa\gamma}{\gamma-1}\,\rho^{\gamma-1} + \frac{\beta^2}{8\pi}\,\rho\right] = 0 ,$$

or

$$\frac{v^2}{2} + \frac{\kappa\gamma}{\gamma-1}\,\rho^{\gamma-1} + \frac{\beta^2}{8\pi}\,\rho = A , \tag{3-33}$$

where A is constant along streamlines, and therefore constant everywhere, since conditions are uniform far upstream. Taking $\gamma = 2$, the Bernoulli equation (33) simplifies to

$$v^2 + \eta\rho = 2A , \tag{3-34}$$

where

$$\eta = 2\kappa + \frac{\beta^2}{8\pi} . \tag{3-35}$$

Using (34), the continuity equation (28) becomes

$$\underset{\sim}{\nabla}\cdot[(2A-v^2)\underset{\sim}{v}] = 0 . \tag{3-36}$$

Now, η has dropped out of this equation, which shows no trace of a magnetic field; it is precisely the equation governing aerodynamic flow (with $\gamma = 2$) past a cylinder. It alone is not sufficient to determine the flow, however, since we have not yet extracted all the information from Euler's equation. If we curl equation (27), we deduce that the vorticity, curl $\underset{\sim}{v}$, is constant along streamlines. This too is uninfluenced by the magnetic field. Thus the velocity is governed by the aerodynamic equations, together with the condition $v_\perp = 0$ at $r = 1$; and hence the solution for $\underset{\sim}{v}$ is the same as in pure aerodynamics (with $\gamma = 2$).

We now ask whether the boundary condition (26) is compatible with the fluid equations. Inserting (31) and (23) into (26), we have

$$\beta \rho (1,\theta) = \sqrt{b^2 - 8\pi \kappa \rho^2} \quad ,$$

or

$$(\beta^2 + 8\pi\kappa) \rho^2(1,\theta) = b^2 \quad ;$$

and b is a constant. So the equation implies that ρ, and therefore (by (34)) v, is independent of θ at $r = 1$. But this is absurd. We know that aerodynamic flow past a blunt body does not have constant speed at the surface; in fact, there is a stagnation point at which the speed vanishes, but it is clearly not everywhere zero. Thus the boundary condition (26) is incompatible with the flow equations, and there is no solution.

Discussion

The relevance of this result to the solar wind is simply

that two-dimensional models, with perpendicular magnetic field, are inadequate to describe its interaction with conducting bodies. This is in contrast with its interaction with the magnetosphere, where there is no additional constraint corresponding to that imposed by Maxwell's equations inside the solid body. Our problem will have to be attacked in three dimensions, which is much harder. It will have been noticed that Theorem I relies on the peculiar topology of the two-dimensional space; we need not expect any corresponding result in three dimensions, and plasma may well flow into the surface of the moon.

It might perhaps seem strange that the problem we have considered has no solution — it looks at first sight like a perfectly reasonable well-posed boundary-value problem, of a kind that is familiar to the physicist. Notice, however, that existence and uniqueness theorems have only been proved for simple equations, such as those of electrodynamics. In fluid mechanics, and, a fortiori, in magnetofluid mechanics, well-posed problems are much rarer than might be supposed by comparison with other branches of physics. An example, obvious to the naked eye, of an ill-posed problem is provided by the flow of an ideal fluid past a perfectly conducting body, with a magnetic field at some non-zero angle to its flow direction. If the body is a sphere, say, then there is a steady solution, in which the field lines slide around the sphere, and thus move past it without entering it. But consider the corresponding two-dimensional problem, flow past a cylinder which is perpendicular to both the velocity and

the magnetic field. Since the perfectly conducting cylinder excludes field, there is no way in which the magnetic field lines can get past it; and therefore, as time goes on, more and more field accumulates on the upstream side, and a steady state is never reached. So the time-independent equations for this problem have no solution, and it is clearly ill-posed. In our problem, the physical reason for the non-existence of a steady state is not so clear, and needs further study to bring it to light.

How can we recognize a well-posed problem? If it is possible in principle to build a piece of apparatus that fulfills the conditions of a problem, then the problem has a solution (though it may not be unique). Now, one can easily construct a machine (such as a wind tunnel) that satisfies the boundary conditions; but I know of no way of building it that ensures that it runs in a steady state. Therefore one cannot be sure that all time-independent problems have solutions. But one can always build a model apparatus satisfying the boundary conditions, start it off in some state, and watch what happens; an initial-value problem <u>is</u> well-posed. If, therefore, one wished to investigate further the problem considered in this section, one might examine an initial-value problem, and see why the system fails to reach an equilibrium state. But that is irrelevant to this dissertation.

IV. INDUCED FIELDS IN THE MOON

4.1 Introduction

In §3.3 we saw that the fields inside a conducting body immersed in a streaming plasma play an important part in determining the flow. We shall now study these interior fields in more detail. We shall develop a theory applicable to a body in direct contact with the interplanetary field — that is to say, a body with no appreciable atmosphere, and no intrinsic field generated in its interior. Our results, like those of Chapter 3, will be mainly applicable to the moon, and Io.

We consider, then, a conducting body immersed in a magnetized plasma. Inside a perfect conductor the field lines are frozen. But in an imperfect conductor, the field diffuses through the medium, with a time constant depending on its size and its conductivity. The diffusion speed in the moon is probably rather slower than the speed at which flux is convected past it by the solar wind, and if this is so, a strong field will build up on the front of the moon (Jokipii, 1965). These matters have been discussed qualitatively by Gold (1966), taking account of the rotation of the moon. This chapter presents a mathematical analysis of the fields induced inside a rotating moon by external sources.

4.2 Theory Without Rotation

In order to test our theoretical machinery on a simple problem, whose behavior is qualitatively understood beforehand, we shall

first consider the diffusion of a uniform field into a stationary sphere. It is not quite as straightforward as one might think.

We suppose the sphere has uniform conductivity σ. Since everything moves much slower than light, we may neglect displacement currents. Then Maxwell's equations, with Ohm's law, give

$$\underset{\sim}{\nabla} \times (\underset{\sim}{\nabla} \times \underset{\sim}{B}) = \underset{\sim}{\nabla} \times (\frac{4\pi\sigma}{c} \underset{\sim}{E}) = - \frac{4\pi\sigma}{c^2} \dot{\underset{\sim}{B}} ,$$

or

$$\underset{\sim}{\nabla} \times (\underset{\sim}{\nabla} \times \underset{\sim}{B}) + \lambda^2 \dot{\underset{\sim}{B}} = 0 , \tag{4-1}$$

and

$$\underset{\sim}{\nabla} \cdot \underset{\sim}{B} = 0 , \tag{4-2}$$

where

$$\lambda^2 = \frac{4\pi\sigma}{c^2} . \tag{4-3}$$

Curl $\underset{\sim}{B}$ and div $\underset{\sim}{B}$ are both finite; therefore $\underset{\sim}{B}$ is continuous at the surface of the sphere.

Equation (1) is a diffusion equation; its solution needs initial and boundary conditions. We wish to simulate the effect of a sudden change in the interplanetary field. At $t = 0$, then, the field vanishes inside our sphere, but is positive outside. The simplest way to formulate this is to impose the boundary condition that $\underset{\sim}{B}$ have a given constant value at the surface; combined with the initial condition that $\underset{\sim}{B} = 0$ in the interior, this gives a well-posed problem for the diffusion equation. We expect the constant field to gradually soak into the sphere.

This strategy is entirely successful for the scalar diffusion equation, for heat flow, for example. But it comes to grief in electromagnetism. The initial-and-boundary-value problem that we have outlined does indeed give a unique solution of (1). Hence there is no freedom left to adjust the solution to satisfy the additional constraint div $\underset{\sim}{B} = 0$. There is no hope of satisfying both equations simultaneously, and the problem has no solution.

There is, in fact, no way that we can set up an experimental model in which the surface magnetic field is under our control. The best we can do is to cover the surface of the sphere with little solenoids, and this determines only the perpendicular component of $\underset{\sim}{B}$. It is thus quite reasonable that it is impossible to prescribe the full surface field, and that our problem is overdetermined. We must find another model.

In the real world, the sphere is surrounded by plasma carrying the magnetic field. This is too difficult for us to handle mathematically. We shall surround our sphere with a vacuum, in which Maxwell's equations are easily solved, and produce the magnetic field by surrounding the system with a very large solenoid. At $t = 0$, we switch on the current in the solenoid. If the current is established in a time ϵ much shorter than the diffusion time of the sphere, then no field penetrates the sphere in that short time;* at $t = 0 + \epsilon$, therefore, the field is zero inside the sphere, uniform at infinity,

---

*Over very short times, the sphere behaves like a superconductor.

and determined everywhere else by Maxwell's equations. If we add the boundary condition $\underset{\sim}{B} \to$ const. at infinity, for all time (which can be physically achieved by keeping constant current flowing through the solenoid), then we should be able to solve the coupled equations (1) and (2), with those boundary conditions, and the initial conditions given at $t = 0 + \epsilon$.

Since div $\underset{\sim}{B} = 0$, (1) may be rewritten

$$\nabla^2 \underset{\sim}{B} - \lambda^2 \underset{\sim}{B} = 0 \ . \tag{4-4}$$

We shall solve this by separating variables. For scalar equations, with spherical geometry, one does this by expanding the independent variable in a series of spherical harmonics. For vector equations, there is a corresponding set of vector spherical harmonics $\underset{\sim}{Y}_{J\ell m}(\theta,\varphi)$; their definition and properties are outlined in Appendix C. They satisfy

$$\nabla^2 \underset{\sim}{Y}_{J\ell m} = \frac{\ell(\ell+1)}{r^2} \underset{\sim}{Y}_{J\ell m} \ . \tag{4-5}$$

We may therefore usefully write

$$\underset{\sim}{B}(r,\theta,\varphi,t) = \Sigma\, u_{J\ell m}(r,t)\, \underset{\sim}{Y}_{J\ell m}(\theta,\varphi) \ , \tag{4-6}$$

where the $u_{J\ell m}(r,t)$ are unknown functions. The $\underset{\sim}{Y}_{J\ell m}$ form a complete orthogonal set, so the expansion (6) is always possible.

It should be noticed that although vector harmonics are discussed in many books, most of those discussions concern radiation problems. If $\underset{\sim}{B}$ has harmonic time dependence $e^{i\omega t}$, then it is possible

to construct a set of divergenceless combinations of $\underset{\sim}{Y}_{J\ell m}$ and radial functions. The solution of the wave equation can then be built up from these combinations, and no further attention need be paid to the condition div $\underset{\sim}{B} = 0$. But for the diffusion equation this method does not work; we must first solve (3), and then apply the constraint (2) to the solution.

Inserting the representation (6) into the equation (4), we get a set of differential equations for the radial functions:

$$\left[\partial_r^2 + \frac{2}{r}\partial_r - \frac{\ell(\ell+1)}{r^2} - \lambda^2\partial_t\right] u_{J\ell m}(r,t) = 0 ,$$

where λ is constant inside the sphere and zero outside. We solve this by introducing the Laplace transform

$$v_{J\ell m}(r,s) = \int_0^\infty u_{J\ell m}(r,t)\, e^{-st}\, dt .$$

Then

$$\left[\partial_r^2 + \frac{2}{r}\partial_r - \frac{\ell(\ell+1)}{r^2} - \lambda^2 s\right] v_{J\ell m}(r,s) = 0, \quad r < 1; \tag{4-7}$$

$$\left[\partial_r^2 + \frac{2}{r}\partial_r - \frac{\ell(\ell+1)}{r^2}\right] v_{j\ell m}(r,s) = 0, \quad r > 1. \tag{4-8}$$

v is continuous at r = 1, the surface of the sphere. For large r, $\underset{\sim}{B} \sim \underset{\sim}{z} = \sqrt{4\pi}\,\underset{\sim}{Y}_{100}$. So for large r, $u_{J\ell m} \sim \sqrt{4\pi}$ if $(J\ell m) = (100)$, and ~ 0 otherwise. Therefore $v_{100}(r,s) \sim \sqrt{4\pi}/s$, and the other $v_{J\ell m} \sim 0$. Hence (100) is the only multipole with non-vanishing boundary conditions; and the equation is homogenous, so all the rest might be expected to vanish. However, the condition div $\underset{\sim}{B} = 0$ couples ℓ to $\ell + 2$, as we shall see, and therefore the solution will contain (120) as well as

(100) multipoles.

The solutions of (7) and (8) that we need are

$$v_o(s) = a(s) \frac{\sinh (r\lambda\sqrt{s})}{r} , \quad r < 1,$$

$$v_o = \frac{\sqrt{4\pi}}{s} + \frac{b(s)}{r} , \quad r > 1;$$

$$v_2 = \alpha(s)\, j_2 (ir\lambda\sqrt{s}) , \quad r < 1,$$

$$v_2 = \frac{\beta(s)}{r^3} , \quad r > 1;$$

where a, b, α, β, are unknown, and j_ℓ is the spherical Bessel function. Continuity at r = 1 gives us two relations between a, b, α, β. The other two that we need come from the divergence condition.

Now, $\underset{\sim}{B} = u_0(r,t) \underset{\sim}{Y}_{100} + u_2 (r,t) \underset{\sim}{Y}_{120}$.

Therefore,

$$\nabla\cdot B = \sqrt{\frac{1}{3}}\, u_0' Y_{10} - \sqrt{\frac{2}{3}} \left(u_2' + \frac{3}{r} u_2\right) Y_{10} = 0 ,$$

using the formulae given in Appendix C. This equation connects $\ell = 2$ with $\ell = 0$, as advertised. Applied to $r < 0$ and $r > 0$, it provides the two further relations between a, b, α, β, needed to fully determine the solution. A routine calculation gives

$$v_o = \frac{\sqrt{4\pi}}{s} , \quad r > 1,$$

$$v_o = \frac{\sqrt{4\pi}\ \sinh (r\lambda\sqrt{s})}{rs \sinh (\lambda\sqrt{s})} , \quad r < 1 ,$$

$$v_2 = -\frac{\lambda\sqrt{2\pi}}{r^3}\,\frac{j_2(i\lambda\sqrt{s})}{\sqrt{s}\,\sinh(\lambda\sqrt{s})} \qquad \text{for } r > 1,$$

$$v_2 = -\lambda\sqrt{2\pi}\,\frac{j_2(ir\lambda\sqrt{s})}{\sqrt{s}\,\sinh(\lambda\sqrt{s})} \qquad \text{for } r < 1\ .$$

These transforms are easily inverted, using the method of Appendix D, giving finally

$$\underset{\sim}{B} = \hat{\underset{\sim}{z}} + \frac{3}{\pi^2 r^3}\sum_1^\infty \frac{1}{n^2}\,e^{-n^2\pi^2 t/\lambda^2}\,(\hat{\underset{\sim}{z}} - 3\,\hat{\underset{\sim}{r}}\cos\theta)\ , \quad r > 1,$$

$$\underset{\sim}{B} = \hat{\underset{\sim}{z}}\left[1 + \frac{2}{\pi r}\sum_1^\infty \frac{(-)^n}{n}\sin(n\pi r)e^{-n^2\pi^2 t/\lambda^2}\right]$$

$$-\,(\hat{\underset{\sim}{z}} - 3\,\hat{\underset{\sim}{r}}\cos\theta)\sum_1^\infty (-)^n\, j_2(n\pi r)e^{-n^2\pi^2 t/\lambda^2}\ , \quad r < 1\ .$$

We see that as $t \to \infty$ the magnetic field relaxes to a uniform distribution, with a characteristic time $\frac{\lambda^2}{\pi^2}$, or λ^2R^2/π^2 in units such that the radius of the sphere is R (instead of 1). This is clearly the correct solution. We can now confidently attack the problem of the rotating sphere.

4.3 Rotating Sphere in Uniform Field

In a moving medium, Ohm's law reads $\sigma[\underset{\sim}{E} + (1/c)\underset{\sim}{v} \times \underset{\sim}{B}] = \underset{\sim}{j}$.

Hence, $\nabla \times \nabla \times \underset{\sim}{B} = \frac{4\pi}{c}\,\nabla \times \underset{\sim}{j} = \frac{4\pi\sigma}{c^2}\left[-\dot{\underset{\sim}{B}} + \nabla \times (\underset{\sim}{v} \times \underset{\sim}{B})\right]$,

or

$$\nabla^2 \underset{\sim}{B} - \lambda^2 \left(\overset{\circ}{\underset{\sim}{B}} - \underset{\sim}{\nabla} \times (\underset{\sim}{v} \times \underset{\sim}{B})\right) = 0, \tag{4-9}$$

where $\underset{\sim}{v} = \underset{\sim}{\Omega} \times \underset{\sim}{r}$ is the velocity of the rotating sphere at the point $\underset{\sim}{r}$.

To simplify this equation, we shall transform to coordinates rotating with the sphere. Then

$$\frac{\partial \underset{\sim}{B}}{\partial t} \rightarrow \frac{\partial \underset{\sim}{B}}{\partial t} - (\underset{\sim}{v} \cdot \nabla)\underset{\sim}{B} + \underset{\sim}{\Omega} \times \underset{\sim}{B} ;$$

the last term takes account of the reshuffling of the components of $\underset{\sim}{B}$ under the rotation. In the new variables, then, (9) becomes

$$\nabla^2 \underset{\sim}{B} - \lambda^2 \left[\dot{\underset{\sim}{B}} - (\underset{\sim}{v} \cdot \underset{\sim}{\nabla})\, \underset{\sim}{B} + \underset{\sim}{\Omega} \times \underset{\sim}{B} - \left\{(\underset{\sim}{B} \cdot \underset{\sim}{\nabla})\, \underset{\sim}{v} - (\underset{\sim}{v} \cdot \underset{\sim}{\nabla})\, \underset{\sim}{B}\right\}\right] .$$

and

$$(\underset{\sim}{B} \cdot \underset{\sim}{\nabla})\, \underset{\sim}{v} = (\underset{\sim}{B} \cdot \underset{\sim}{\nabla})(\underset{\sim}{\Omega} \times \underset{\sim}{r}) = \underset{\sim}{\Omega} \times \underset{\sim}{B} ;$$

so

$$\nabla^2 \underset{\sim}{B} - \lambda^2 \dot{\underset{\sim}{B}} = 0 \tag{4-10}$$

in the rotating coordinates.

Notice that we have simply made a change of independent variable in (9) to reduce it to (10); it is not a Lorentz transformation. I do not claim that the $\underset{\sim}{B}$ of equation (10) is the true magnetic field observed in the rotating frame (though this can be shown to be true, if $v \ll c$), nor that the Maxwell equations used to derive (1) are valid in the rotating frame (which is false); I claim only that the solution of (10) is a function which, when transformed back into fixed axes, gives correctly the magnetic field in those axes.

We have reduced our problem to the solution of the same equations as in §4.2, and we will solve them by the same method. The boundary conditions, however, are more complicated. We choose the z axis to be the rotation axis, and apply at infinity a uniform field at an angle α to it. Thus in the space-fixed axes,

$$\begin{aligned} \underset{\sim}{B}^{f}(\infty) &= \hat{\underset{\sim}{z}} \cos\alpha + \hat{\underset{\sim}{x}} \sin\alpha \\ &= \sqrt{4\pi}\left[\cos\alpha\, \underset{\sim}{Y}_{100} + \sqrt{\tfrac{1}{2}} \sin\alpha\, (\underset{\sim}{Y}_{101} - \underset{\sim}{Y}_{10-1})\right]. \end{aligned}$$

In the rotating frame the boundary conditions are time-dependent. At time t, the rotating axes are at an angle ωt to the fixed axes. Since a rotation about the z axis, through angle φ, multiplies $\underset{\sim}{Y}_{J\ell m}$ by $e^{im\varphi}$, we have, in the rotating frame,

$$\underset{\sim}{B} \sim \sqrt{4\pi}\left[\cos\alpha\, \underset{\sim}{Y}_{100} + \frac{1}{\sqrt{2}} \sin\alpha\, (e^{i\omega t}\, \underset{\sim}{Y}_{101} - e^{-i\omega t}\, \underset{\sim}{Y}_{10-1})\right],$$

for large r. The calculation is now exactly parallel to that of §4.2; we shall give only the results:

$$u_{100} = \sqrt{4\pi}\cos\alpha,\quad u_{10\pm1} = \pm\sqrt{2\pi}\sin\alpha\, e^{\pm i\omega t} \qquad , r > 1,$$

$$u_{100} = \frac{\sqrt{4\pi}\cos\alpha}{r}\left[r + \frac{2}{\pi}\sum \frac{(-)^n}{n} \sin n\pi r\, e^{-n^2\pi^2 t/\lambda^2}\right], \quad r < 1$$

$$u_{10\pm1} = \pm\frac{\sqrt{2\pi}\sin\alpha}{r}\left[\frac{\sinh(r\lambda\sqrt{\pm i\omega})}{\sinh(\lambda\sqrt{\pm i\omega})} e^{\pm i\omega t} + \right.$$

$$\left. + 2\pi\sum (-)^n \frac{n \sin n\pi r}{n^2\pi^2 \pm i\omega\lambda^2} e^{-n^2\pi^2 t/\lambda^2}\right] \qquad , r < 1,$$

$$u_{120} = \frac{\sqrt{2\pi}\cos\alpha}{r^3}\,\frac{6}{\pi^2}\sum\frac{1}{n^2}\,e^{-n^2\pi^2 t/\lambda^2} \qquad , \quad r > 1$$

$$u_{12\pm1} = \mp\frac{\sqrt{\pi}\sin\alpha}{r^3}\left[\frac{\lambda\sqrt{\pm i\omega}\; j_2(i\lambda\sqrt{\pm i\omega})}{\sinh(\lambda\sqrt{\pm i\omega})}\,e^{\pm i\omega t} - 6\sum\frac{e^{-n^2\pi^2 t/\lambda^2}}{n^2\pi^2 \pm i\omega\lambda^2}\right], \quad r > 1$$

$$u_{120} = -\sqrt{8\pi}\,\cos\alpha\,\Sigma\,(-)^n\, j_2(n\pi r)\, e^{-n^2\pi^2 t/\lambda^2} \qquad , \quad r < 1$$

$$u_{12\pm1} = \mp\sqrt{\pi}\,\sin\alpha\left[\lambda\sqrt{\pm i\omega}\,\frac{j_2(ir\lambda\sqrt{\pm i\omega})}{\sinh(\lambda\sqrt{\pm i\omega})}\,e^{\pm i\omega t} + \sum\frac{(-)^n n^2\pi^2}{n^2\pi^2 \pm i\omega\lambda^2}\,2j_2(n\pi r)\,e^{-n^2\pi^2 t/\lambda^2}\right]$$

$$. \quad r < 1 \;.$$

These are complicated formulae. However, they contain a dimensionless parameter, $R\lambda\sqrt{\omega}$, where R is the radius of the sphere (=1 in the units used for the calculation). For very small or very large values of this parameter, the equations simplify. If it is very small, then the diffusion time is much shorter than the rotation period, and the rotation has only a small effect on the magnetic field. To a first approximation, the externally applied field simply diffuses into the sphere, and the problem reduces to that of §4.2. But if the rotation is much faster than the diffusion, then more interesting phenomena appear.

$R\lambda\sqrt{\omega} \sim 40\sqrt{\sigma}$, where σ is the conductivity in mho/cm. We have, of course, no direct information about the conductivity of the moon. However, studies of geomagnetic variations have told us something about the conductivity of the earth's mantle, and it seems reasonable to suppose that the moon is made of similar materials. At a depth of

600 km. in the earth, $\sigma > 10^{-12}$ mho/cm.; at 1000 km. it is probably well over 10^{-1} mho/cm. (Runcorn 1956). Thus $R\lambda\sqrt{\omega} \gg 1$ is a reasonable approximation, and we shall use it from now on (see also the remarks at the end of the chapter.)

The Steady State

Let us first consider the axial component of the field: the terms in cos α (α is the angle between the applied field and the rotation axis). These terms are independent of ω, and are indeed identical to the solution of §4.2 for any value of the parameter $R\lambda\sqrt{\omega}$. The rotation has no effect on the axial component of a uniform applied field. This is a reasonable result, considering the complete axial symmetry of such a field.

We now consider the effect of an applied field in the equatorial plane: the sin α terms. Transforming to the space-fixed axes ($\varphi \to \varphi - \omega t$) we find that the steady-state interior field (after the transients have died away) is

$$\frac{e^{-(1-r)/r\delta}}{2r}\left[-\hat{\underset{\sim}{z}}\cos\theta\sin\theta\cos\Psi - 3\hat{\underset{\sim}{\rho}}\sin^2\theta\cos\Psi + \hat{\underset{\sim}{\varphi}}\sin\Psi\right], \tag{4-11}$$

where

$$\Psi \equiv \varphi - \frac{(1-r)}{\delta},$$

$$\delta \equiv \frac{1}{\lambda}\sqrt{\frac{2}{\omega}},$$

and $\hat{\underset{\sim}{\rho}}$ is the radial unit vector in cylindrical coordinates.

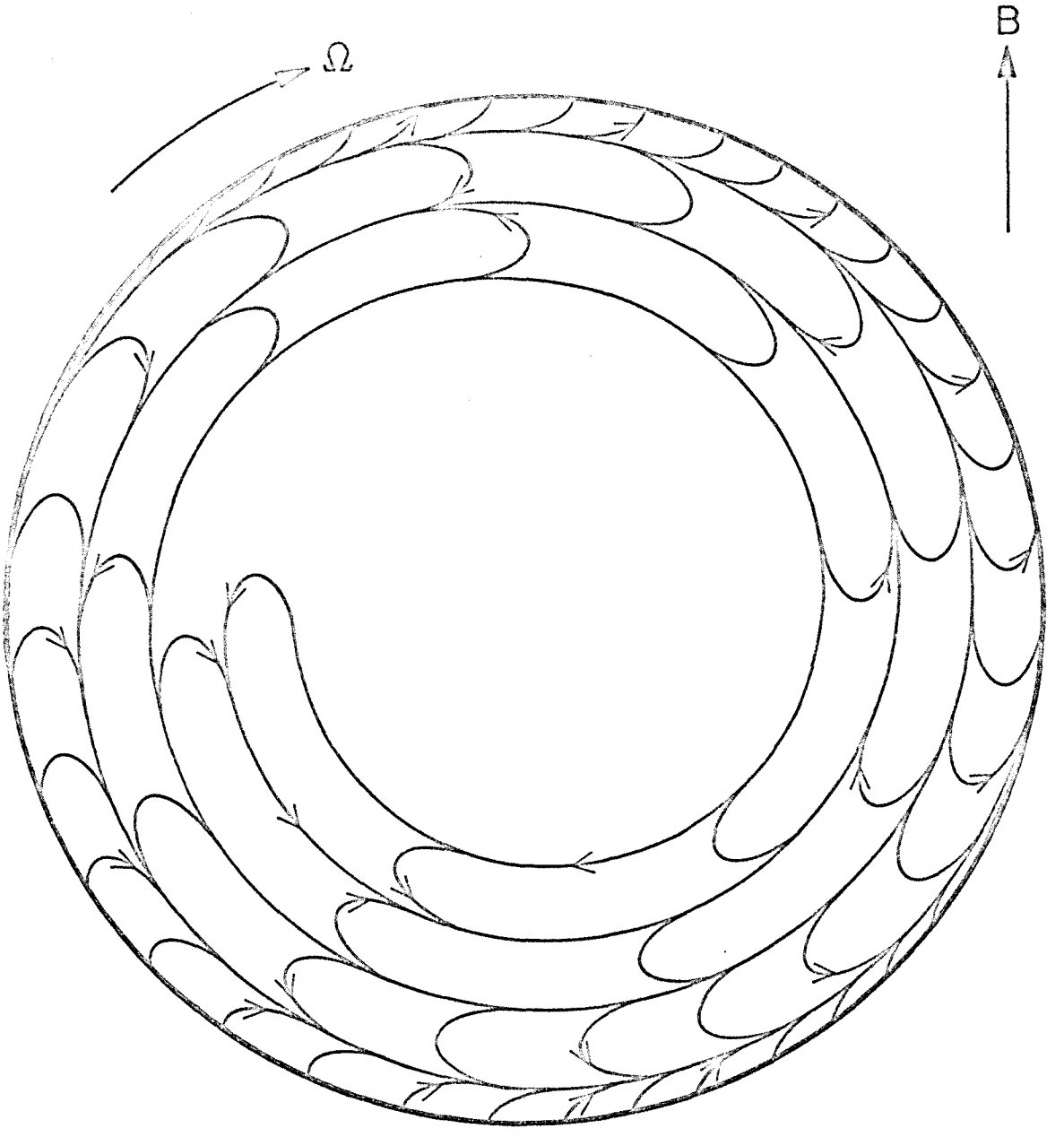

Figure 9. Magnetic field on the equatorial plane of a rapidly spinning sphere. Radial scale exaggerated.

We have assumed $\delta \ll 1$, and $\delta/r \ll 1$. (11) is therefore not valid for very small r — which is just as well, since it diverges at r = 0.

We see from (11) that the field decreases rapidly with depth, and is negligible everywhere except in a layer of thickness δ at the surface. This was predicted by Gold (1966); however, we shall see that the interior is free of toroidal fields only if the applied field is uniform. In order to understand this result, imagine a little arrow, representing the magnetic field vector, embedded in the sphere. As the sphere rotates, the field vector rotates with it (almost frozen — in fields), and also diffuses inwards slowly, thus traveling along a spiral (see Figure 9). By the time the sphere has rotated through 180°, this field vector is pointing in the opposite direction to the external field, which now begins to soak in above it. In this way a spiral structure of fields in alternating directions is built up near the surface. As it diffuses downwards, the reversed layers diffuse into each other, and finally cancel out almost completely. The spiral structure is clear in the formula (11): the field is constant in direction (in cylindrical coordinates) along curves of constant ψ, which are Archimedes spirals, very tightly wound.

Transients

For an axial applied field, the solution is, as we saw, unaffected by the rotation. For a field applied in the equatorial plane ($\alpha = \pi/2$), the solution for the external field on the equatorial plane, for $\delta \ll 1$, is

$$\hat{\underset{\sim}{\rho}} \left[\cos\varphi - 12\,\delta^2 \sin(\varphi-\omega t) \sum e^{-n^2\pi^2 t/\lambda^2}\right]$$

$$+ \hat{\underset{\sim}{\varphi}} \left[-\sin\varphi + 6\delta^2 \cos(\varphi-\omega t) \sum e^{-n^2\pi^2 t/\lambda^2}\right] \quad .$$

This is valid unless t is so small that the high transients with $n \gtrsim 1/\delta$ are important. We see that the transients are smaller than the main field by a factor δ^2.

This result is true when the applied field is uniform. We have seen that in this case it is excluded from the interior of a rapidly rotating sphere, which thus behaves somewhat like a superconductor. Since our initial condition was precisely the static field configuration around a superconductor, it is not surprising that only a small adjustment is needed for the exterior field to settle down to a steady state.

4.4 Non-uniform Applied Fields

The solar wind is continuously convecting magnetic flux towards the moon. If the moon is highly conducting, a strong field will be built up on the upstream side, compared with the fields at other parts of the lunar surface. This ought to be incorporated into our model, and we shall therefore modify the boundary conditions.

If the applied field is axial, then, as we have seen, the problem is unaffected by the peculiarities of vectors, and the solution resembles heat conduction: the interior field will be uniform and equal to the average surface field, except in a thin layer at the surface, in which it adjusts to the non-uniform boundary condition.

We shall consider in detail the more interesting case of applied fields in the equatorial plane. Instead of demanding that the field be constant at large distances, we shall say that the distant field is (roughly) in the x-direction, but is greater for large positive y than for large negative y. This is easily done by adding to the constant field a new field, whose lines of force are circles, centered on the origin, reinforcing the original field at one side, and partly canceling it out at the other. $\underset{\sim}{Y}_{110}=i\sqrt{(3/8\pi)}\ \sin\theta\ \underset{\sim}{\varphi}$ is a suitable multipole to represent this field: it gives maximum distortion at the equator, and none at the poles, which is roughly what we expect for the fields around the moon. The corresponding solution of the vacuum Maxwell equations is $r^{-2}\ \underset{\sim}{Y}_{110}$. Our boundary condition, in the space-fixed axes, is thus

$$\underset{\sim}{B} \sim \sqrt{2\pi}\ (\underset{\sim}{Y}_{101} - \underset{\sim}{Y}_{10-1}) + \frac{id}{r^2}\ \underset{\sim}{Y}_{110}$$

for large r, where d is a (real) parameter, measuring the amount of distortion — the difference between the upstream and downstream surface fields.

The solution of the new problem is the same as that of §4.3, except for the addition of terms involving $\underset{\sim}{Y}_{110}$. These are easily calculated, since div $[f(r)\ \underset{\sim}{Y}_{110}] = 0$ for any f(r), and there is therefore no need to explicitly impose the divergence condition. The resulting addition to the magnetic field is, for $r < 1$,

$$-d\sqrt{\frac{3}{8\pi}}\left\{r + \sum_{1}^{\infty} \frac{2}{z_n}\ \frac{j_1(rz_n)}{j_1'(z_n)}\ e^{-z_n^2 t/\lambda^2}\right\} \sin\theta\ \underset{\sim}{\hat{\varphi}},$$

where z_n is the n^{th} zero of $j_1(z)$. The external field is constant in time.

Now, for $t = 0$ and $r < 1$, the internal field must vanish. But as time goes on, an azimuthal field soaks into the sphere, and when the transients have died away the sphere is filled with an azimuthal field, of strength proportional to radius, and matching at the surface the imposed external field. Upon this is superimposed the spiral structure in the thin surface layer discussed in §4.3.

4.5 Discussion

When the applied field is non-uniform, and in the equatorial plane, we may understand the steady-state field structure on the basis of the discussion of Figure 9. The intertwining layers of alternating fields now have unequal strengths: since there is greater applied field on the upstream side, the layer starting from that side is stronger than the other. Hence when the layers diffuse into each other, they do not cancel out completely; a toroidal field is left throughout the sphere, proportional (and equal at the surface) to the difference between the applied fields at the front and back of the sphere.

The general picture to which we have been led may be summed up as follows — always under the assumption that $R\lambda\sqrt{\omega} \gg 1$. If the interplanetary field has been constant for a long time (longer than the diffusion time), then its mean North-South component completely penetrates the moon. A toroidal field, proportional to the degree of magnetic compression at the upstream side, also fills the interior of

the moon; and in a thin skin near the surface is a spiral structure like that of Figure 9.

When the interplanetary field changes, the new values of the axial and azimuthal fields will gradually sink into the moon. If the diffusion time is longer than the time between changes in the interplanetary field, then (as Gold (1966) remarks) there will be remnants of older North-South fields in the interior; indeed, there will be a sequence of layers of alternating North and South fields, displaying the history of the fluctuating North component of the interplanetary field. Superimposed upon this will be a similar shell structure of toroidal fields. The conductivity, and therefore, the diffusion time, almost certainly increases considerably with depth; these fossil magnetic fields will therefore be frozen into the central part of the moon, even if they have diffused away in the equatorial regions.

It seems rather likely that the conductivity in the outer layers of the moon is low (see the values quoted in §4.3; also Tozer and Wilson, 1967), and the diffusion time there is short, compared to the rotation period. This suggests (as Tozer and Wilson remark) that one might usefully consider a two-layer model of the moon, in which the outer layer is approximated by an insulator. The theory of this chapter applies to such a model, if the radius of the sphere is taken to mean the radius of the inner, conducting part; the induced fields will appear in the core, just as if it were not surrounded by an insulating shell.

APPENDIX A

THE EVAPORATION MODEL

The simplest possible approach to the solar wind is to treat it as particles that have boiled off the surface of the sun, and travel outwards uninfluenced by collisions, magnetic fields, or any other collective effects. Early work on this model predicted very low velocities for the wind. But recently the idea has been revived, and it has been shown that the energy dependence of the Coulomb collision cross-section makes it easier for fast particles to escape; Brandt and Cassinelli (1966) have been able to construct models in reasonable agreement with the observed gross average properties of the wind.

Now, in §2.3 we show that the spiral magnetic field plays an important role in the particle dynamics; conservation of the magnetic moment of the particles leads to considerable cooling of the transverse temperature. We shall show here that completely ignoring the magnetic field leads to results more accurate than might at first be expected.

As in §2.3 we shall suppose that the wind is collision-dominated within a distance D from the sun, and collisionless beyond, and that the particles travel in straight lines outwards from r = D (solar gravity is negligible for $D \gtrsim .1$ A.U.). We assume isotropy of the velocity distribution at r = D, and complete spherical symmetry of the problem.

Consider the velocity distribution at a point P, at a distance r from the center of the sun. All the velocities are clearly

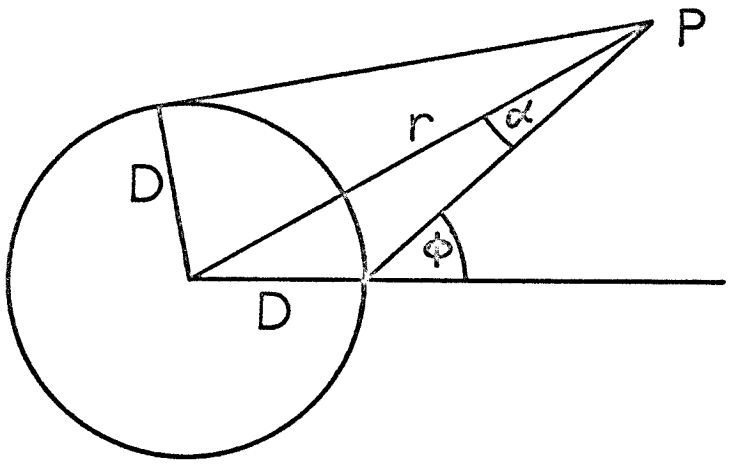

Figure 10

Geometry of the Evaporation Model

confined within a cone, of half-angle $\sin^{-1}(r/D)$ (see Fig. 10). Hence the distribution is anisotropic; the spread in transverse velocity is much reduced at large distances, while the radial velocity distribution is not much affected. This reminds us of the results, in §2.3, for particles in a radial magnetic field. In this case, too, the velocity vectors all lie within a cone pointing away from the sun, but for a different reason: conservation of the magnetic moment implies that the pitch angle of a particle decreases as it travels outwards; the pitch angles of all particles arriving at r have been reduced by this mechanism, and are all less than some limiting value. And this angle is precisely $\sin^{-1}(r/D)$.

This is curious. Let us examine the velocity distribution more closely. Consider the motion of a particle emitted from D at an angle φ to the normal, with no magnetic field. If its velocity is at an angle α to the radial direction at heliocentric distance r, then

(see Fig. 10)

$$\sin \alpha = \frac{D \sin \varphi}{r} \quad . \qquad \text{(A-1)}$$

Now, both the definition of α and its r-dependence according to (1) are the same as for the pitch angle of a particle moving in an inverse-square magnetic field. So if the orbits are described by giving $v(r)$ and $\alpha(r)$, and ignoring the third component, then they are the same in the two cases. It follows that if the models are spherically symmetric (so that the third component is irrelevant), then their distribution functions are identical. Nature conspires to cancel out the error committed by ignoring the magnetic field.

One might perhaps try to understand this result along the following lines. The dynamics of particles in a radial magnetic field is independent of the absolute strength of the field: if B is everywhere halved, the distribution function is unchanged. Therefore it stays the same in the limit $B \to 0$, Q.E.D. However, it is not that simple. Our calculation of the orbits was based on the invariance of the magnetic moment. This is valid only if the gyroradius is much less than the scale length of the field. As $B \to 0$, the gyroradius $\to \infty$, while the scale length stays constant: therefore the adiabatic invariance, and with it the above argument, breaks down. The equivalence of the two models seems to be just a delightful coincidence.

APPENDIX B

SURFACE CONDITIONS ON CONDUCTING BODIES

Two Dimensions

Consider a uniformly conducting body in a steady electromagnetic field. Maxwell's equations in the interior of the body impose certain constraints on the boundary values of the fields, which it is the purpose of this appendix to discover.

We consider first a two-dimensional problem, with $\underset{\sim}{B} = B(x,y)\hat{\underset{\sim}{z}}$, and a cylindrical conductor. In a steady state, curl curl $\underset{\sim}{B} = (4\pi\sigma/c) \times$ curl $\underset{\sim}{E} = 0$. So

$$\nabla^2 B = 0 \quad . \tag{B-1}$$

And div $\underset{\sim}{E}$ = div $\underset{\sim}{J}/\sigma = - \dot{\rho}/\sigma = 0$ in a steady state; and curl $\underset{\sim}{E} = 0$ of course; so $\underset{\sim}{E}$ may be derived from a scalar potential ψ satisfying Laplace's equation

$$\nabla^2 \psi = 0 \quad . \tag{B-2}$$

The general solution of (B-1) that is regular at the origin is

$$B(r,\theta) = \sum_{-\infty}^{\infty} \beta_n r^{|n|} e^{ni\theta} \quad , \tag{B-3}$$

where β_n are arbitrary constants.

Let b_n be the Fourier coefficients of the boundary value $B(1,\theta)$ of B. A knowledge of all b_n is equivalent to knowledge of $B(1,\theta)$. Putting r = 1 in (3) gives $\beta_n = b_n$, and so

$$B(r,\theta) = \sum_{-\infty}^{\infty} b_n r^{|n|} e^{ni\theta} \quad . \tag{B-4}$$

Similarly, the general solution of (B-2) is

$$\psi(r,\theta) = \sum \psi_n r^{|n|} e^{ni\theta} ,$$

where ψ_n are arbitrary constants, related to the boundary values of the electric field. Now, at the surface of a conductor, $E_\perp$ will not in general be continuous, since there may be charges on the surface. Therefore the boundary value of $E_\perp$ is unrelated to the interior fields. But $E_\parallel$ must be continuous, and so $E_\parallel$ calculated from (B-4) must agree with the boundary value $e(\theta) \equiv E_\theta(1,\theta)$. Thus

$$\sum \psi_n in\, e^{ni\theta} = e(\theta),$$

or

$$in\psi_n = e_n,$$

where e_n are the Fourier components of $e(\theta)$. So

$$\psi(r,\theta) = - i \sum{}' \frac{e_n}{n} r^{|n|} e^{ni\theta} , \qquad \text{(B-5)}$$

where $\sum'$ means a sum omitting the n = 0 term; it is a constant, and may therefore be dropped from the potential. We have now expressed the fields in terms of their boundary values. We now demand that they satisfy

$$\nabla \times \underset{\sim}{B} = \frac{4\pi}{c} \sigma \underset{\sim}{E} ,$$

or

$$\frac{1}{r} \frac{\partial B}{\partial \theta} = \frac{4\pi\sigma}{c} \frac{\partial \psi}{\partial r} \qquad \text{(B-6)}$$

and

$$- \frac{\partial B}{\partial r} = \frac{4\pi\sigma}{c} \left(\frac{1}{r}\right) \frac{\partial \psi}{\partial \theta} \qquad \text{(B-7)}$$

Inserting the representations (B-4) and (B-5) into these conditions

gives us

$$\sum{}' \text{in} b_n r^{|n|-1} e^{ni\theta} = \frac{4\pi\sigma}{c} \sum{}' - i \frac{|n|}{n} e_n r^{|n|-1} e^{ni\theta} ;$$

this is necessary and sufficient for both (B-6) and (B-7). So

$$n\, b_n = - \epsilon(n) \frac{4\pi\sigma}{c} e_n ,$$

where $\epsilon(n)$ is the step function $|n|/n$; or

$$|n|\, b_n = - \frac{4\pi\sigma}{c} e_n \quad . \tag{B-8}$$

This is the condition imposed on the boundary values by Maxwell's equations in the interior. An alternative form of (B-8) is

$$b(\theta) = b_0 - \frac{4\pi\sigma}{c} \sum{}' \frac{1}{|n|} e_n e^{ni\theta}$$

where b_0 is an arbitrary constant, the n = 0 term which is not constrained by the condition (B-8). Now,

$$e_n = \frac{1}{2\pi} \oint d\alpha\, e(\alpha)\, e^{-ni\alpha} ,$$

so

$$b(\theta) = b_0 - \frac{2\sigma}{c} \oint d\alpha\, e(\alpha) \sum{}' \frac{1}{|n|} e^{ni(\theta-\alpha)} .$$

But

$$\sum{}' \frac{1}{|n|} e^{ni\varphi} = \sum_1^\infty \frac{1}{n} (e^{ni\varphi} + e^{-ni\varphi}) = i \int d\varphi \sum_1^\infty (e^{ni\varphi} - e^{-ni\varphi}).$$

These are geometric series and easily summed, giving us, after some juggling

$$= -2 \log | 2 \sin (\varphi/2)| .$$

Hence

$$b(\theta) = b_o + \frac{4\sigma a}{c} \oint d\alpha\, e(\alpha) \log|2 \sin (\tfrac{\alpha-\theta}{2})| ; \tag{B-9}$$

a is the radius of the cylinder, which we took to be 1, but which should be restored to keep the dimensions right.

Three Dimensions

We shall now do a similar calculation with spherical geometry. As before, we have

$$\nabla^2 \psi = 0 \quad , \tag{B-10}$$

$$\nabla^2 \underset{\sim}{B} = 0 \quad . \tag{B-11}$$

The general solution of (B-10) which is regular at the origin is

$$\psi(r,\theta,\varphi) = \sum \psi_{\ell m} r^{\ell} Y_{\ell m}(\theta,\varphi) \quad , \tag{B-12}$$

where $\psi_{\ell m}$ are constants, and $Y_{\ell m}$ are the spherical harmonics. $\psi_{\ell m}$ are the coefficients of the spherical harmonic expansion of the potential at the surface, knowledge of which is equivalent to knowledge of the tangential electric field at the surface.

The analog of (B-12) for the vector field $\underset{\sim}{B}$ is

$$\underset{\sim}{B}(r,\theta,\varphi) = \sum b_{J\ell m} r^{\ell} \underset{\sim}{Y}_{J\ell m}(\Omega) \quad , \tag{B-13}$$

where the vector spherical harmonics $\underset{\sim}{Y}_{J\ell m}$ are the vector analogs of $Y_{\ell m}$; their definition and properties are outlined in Appendix C. Again, $b_{J\ell m}$ are the coefficients in the multipole expansion of the surface magnetic field; knowing all $b_{J\ell m}$ is equivalent to knowing $\underset{\sim}{B}(1,\theta,\varphi)$ (note that for each ℓ, m, there are three values of J, corresponding to the three components of the vector).

We now impose Maxwell's equations upon the representations (B-12), (B-13), beginning with div $\underset{\sim}{B} = 0$. Using the formulae of Appendix C we have

$$\underset{\sim}{\nabla}\cdot(r^{\ell}\,\underset{\sim}{Y}_{\ell\ell m}) = 0 \quad ,$$

$$\underset{\sim}{\nabla}\cdot(r^{\ell-1}\,\underset{\sim}{Y}_{\ell,\ell-1,m}) = 0 \quad ,$$

$$\underset{\sim}{\nabla}\cdot(r^{\ell+1}\,\underset{\sim}{Y}_{\ell,\ell+1,m}) \neq 0 \quad .$$

Therefore $\underset{\sim}{B}$ must not contain any $(\ell, \ell+1, m)$ multipoles:

$$b_{\ell,\ell+1,m} = 0 \quad , \tag{B-14}$$

This is the first constraint imposed by Maxwell's equations. We also have

$$\underset{\sim}{\nabla} \times \underset{\sim}{B} = (4\pi/c)\underset{\sim}{j} = (4\pi\sigma/c)\underset{\sim}{E}$$

or

$$\underset{\sim}{\nabla} \times \underset{\sim}{B} = (4\pi\sigma/c)\ \underset{\sim}{\nabla}\psi \tag{B-15}$$

Now

$$\underset{\sim}{\nabla}(r^{\ell}Y_{\ell m}) = \sqrt{\ell(2\ell+1)}\ r^{\ell-1}\underset{\sim}{Y}_{\ell,\ell-1,m} \ ,$$

$$\underset{\sim}{\nabla} \times (r^{\ell}\underset{\sim}{Y}_{\ell\ell m}) = i\sqrt{(\ell+1)(2\ell+1)}\ r^{\ell-1}\underset{\sim}{Y}_{\ell,\ell-1,m},$$

$$\underset{\sim}{\nabla} \times (r^{\ell-1}\,\underset{\sim}{Y}_{\ell,\ell-1,m}) = 0 \quad ,$$

(see Edmonds (1957) p.84). Applying these formulae to (B-15), we have

$$i\sum b_{\ell\ell m}\sqrt{(\ell+1)(2\ell+1)}\,r^{\ell-1}Y_{\ell,\ell-1,m} = \frac{4\pi\sigma}{c}\sum\psi_{\ell m}\sqrt{\ell(\ell+1)}\,r^{\ell-1}\underset{\sim}{Y}_{\ell,\ell-1,m}$$

Since the $Y_{J\ell m}$ are orthogonal, we deduce

$$i\sqrt{\ell+1}\ b_{\ell\ell m} = \frac{4\pi\sigma}{c}\ \sqrt{\ell}\ \ \psi_{\ell m} \tag{B-16}$$

(this is dimensionally correct). (B-14) and (B-16) are the constraints

imposed by Maxwell's equations upon the steady-state fields at the surface of a uniform sphere. If the magnetic field is given, then it must satisfy the constraint (B-14); and it completely determines the electric potential. If the potential is given, it provides half the information needed to construct B.

APPENDIX C

THE VECTOR SPHERICAL HARMONICS

This mathematical apparatus was introduced into physics for the sake of atomic and nuclear theory, and therefore most accounts of it are written in the language of quantum mechanics (an exception is Part I of Fano and Racah, 1959). However, the theory itself (the theory of spherical tensors) is pure mathematics, and is as useful for classical fields as for quantum wave functions (e.g., Mathews, 1962). Since there are full accounts of the subject in books such as Edmonds (1957), I will give here only the definitions of the vector harmonics, and those properties that are needed for our calculations.

The conventional spherical harmonics are defined by

$$Y_{\ell m}(\theta,\varphi) = \left[\left(\frac{2\ell+1}{4\pi}\right)\ \frac{(\ell-m)!}{(\ell+m)!}\right]^{1/2} P_{\ell}^{m}(\cos\theta)\ e^{im\varphi}\ ,$$

where $P_{\ell}^{m}(x)$ is the familiar associated Legendre function as defined in Magnus and Oberhettinger, and Condon and Shortley. This P_{ℓ}^{m} differs by a factor $(-)^{m}$ from that of Edmonds, but in all other respects (including the definition of $Y_{\ell m}$), our conventions agree with both Edmonds and Condon and Shortley.

The spherical harmonics satisfy

$$Y_{\ell,-m} = Y_{\ell m}^{*}(-)^{m}\ ,$$

$$\int Y_{\ell m}(\Omega)\ Y_{\ell' m'}(\Omega)\ d\Omega = \delta_{\ell\ell'}\ \delta_{mm'},\ \text{where } d\Omega = \sin\theta\ d\theta d\varphi\ .$$

In place of the orthonormal triad $\hat{\underset{\sim}{x}}$, $\hat{\underset{\sim}{y}}$, $\hat{\underset{\sim}{z}}$, we introduce the spherical basis vectors

$$\hat{\underset{\sim}{\chi}}_0 \equiv \hat{\underset{\sim}{z}}, \quad \hat{\underset{\sim}{\chi}}_{\pm 1} \equiv \sqrt{\frac{1}{2}} \left(\mp \hat{\underset{\sim}{x}} - i\hat{\underset{\sim}{y}}\right) ,$$

$\hat{}$ denoting a unit vector, as usual. They satisfy

$$\hat{\underset{\sim}{\chi}}_s \cdot \hat{\underset{\sim}{\chi}}_t^* = \delta_{st}, \quad \hat{\underset{\sim}{\chi}}_s^* = (-)^s \hat{\underset{\sim}{\chi}}_{-s} ,$$

$$\hat{\underset{\sim}{\chi}}_s \times \hat{\underset{\sim}{\chi}}_t = i \in_{stu} \hat{\underset{\sim}{\chi}}_u^* .$$

We define the vector spherical harmonics by

$$\underset{\sim}{Y}_{J\ell m} = \sum_{s=-1}^{1} C(\ell, m - s; 1, s; J, m)\, Y_{\ell, m-s}\, \hat{\underset{\sim}{\chi}}_s ,$$

where the $C(\ell_1, m_1; \ell_2, m_2; J, m)$ are a set of numerical coefficients (the Clebsch-Gordan coefficients), the values of which can be found in Edmonds, and most books on non-elementary quantum mechanics.

The vector harmonics satisfy

$$\nabla^2 \underset{\sim}{Y}_{J\ell m} = \frac{\ell(\ell + 1)}{r^2} \underset{\sim}{Y}_{J\ell m} .$$

This is true for $\underset{\sim}{Y}_{J\ell m}$ simply because $Y_{\ell m}$ satisfies the same equation; it does not depend upon any properties of the Clebsch-Gordan coefficients. The virtue of these coefficients lies in the fact that the $\underset{\sim}{Y}_{J\ell m}$ constructed using them have simple transformation properties under rotation. Indeed, a coordinate rotation about the z axis, through φ, simply multiplies $\underset{\sim}{Y}_{J\ell m}$ by $e^{im\varphi}$; and there are corresponding (though not quite so simple) results for rotation about other axes. The unitarity properties of the Clebsch-Gordan coefficients lead to orthonormality of the vector harmonics:

$$\oint d\Omega\, \underset{\sim}{Y}_{J\ell m}(\Omega) \cdot \underset{\sim}{Y}_{J'\ell'm'}(\Omega) = \delta_{\ell\ell'} \delta_{JJ'} \delta_{mm'} .$$

We shall need to know the divergence of the harmonics:

$$\underset{\sim}{\nabla}\cdot[u(r)\ \underset{\sim}{Y}_{\ell,\ell+1,m}] = -\left[\frac{\ell+1}{2\ell+1}\right]^{1/2}\left[\frac{d}{dr}+\frac{\ell+2}{r}\right] u\ Y_{\ell m}\ ,$$

$$\underset{\sim}{\nabla}\cdot[u(r)\ \underset{\sim}{Y}_{\ell\ell m}] = 0\ ,$$

$$\underset{\sim}{\nabla}\cdot[u(r)\ \underset{\sim}{Y}_{\ell,\ell-1,m}] = \left[\frac{\ell}{2\ell+1}\right]^{1/2}\left[\frac{d}{dr}-\frac{\ell-1}{r}\right] u\ Y_{\ell m}\ .$$

More information will be found in Edmonds.

The first few harmonics are:

$$\underset{\sim}{Y}_{010} = -\frac{1}{\sqrt{4\pi}}\ \underset{\sim}{\hat{r}}\ ,$$

$$\underset{\sim}{Y}_{100} = \frac{1}{\sqrt{4\pi}}\ \underset{\sim}{\hat{z}}\ ,$$

$$\underset{\sim}{Y}_{10\pm1} = \mp\frac{1}{\sqrt{8\pi}}\ (\underset{\sim}{\hat{x}} \pm i\underset{\sim}{\hat{y}})\ ,$$

$$\underset{\sim}{Y}_{110} = i\sqrt{\frac{3}{8\pi}}\ \sin\theta\ \underset{\sim}{\hat{\varphi}}\ ,$$

$$\underset{\sim}{Y}_{11\pm1} = -\sqrt{\frac{3}{16\pi}}\ \left[\sin\theta\ e^{\pm i\varphi}\ \underset{\sim}{\hat{z}} - \cos\theta\ (\underset{\sim}{\hat{x}} \pm i\underset{\sim}{\hat{y}})\right]\ .$$

APPENDIX D

LAPLACE INVERSION

To illustrate the methods used to invert the Laplace transforms of sections 4.2 and 4.3, we shall derive the inverse of

$$\frac{\lambda\sqrt{s}}{s - i\omega}\ \frac{j_2(ir\lambda\sqrt{s})}{\sinh(\lambda\sqrt{s})} \quad .$$

It is

$$\frac{1}{2\pi i}\int_{c-i\infty}^{c+i\infty} e^{st}\, ds\, \frac{\lambda\sqrt{s}}{s - i\omega}\ \frac{j_2(ir\lambda\sqrt{s})}{\sinh(\lambda\sqrt{s})} \quad ,$$

where $c >$ Real part of any singularity of the integrand.

Now, the integrand appears to have a branch point. But j_2 is an even function of its argument, and so is $\lambda\sqrt{s}/\sinh(\lambda\sqrt{s})$. Therefore, when $s \to -s$, the integrand is unchanged. In spite of appearances, therefore, it is a single-valued analytic function of s, with poles at $s = i\omega$, and $s = -n^2\pi^2/\lambda^2$ (the zeros of $\sinh \lambda\sqrt{s}$). As $s \to 0$, $\lambda\sqrt{s}/\sinh(\lambda\sqrt{s}) \to 1$, so the integrand is analytic there.

The e^{st} factor ensures that we can complete the contour of integration with a large semicircle on the left, without changing the integral; it then becomes the sum of the residues:

$$\frac{\lambda\sqrt{\omega}\ j_2(ir\lambda\sqrt{\omega})}{\sinh(\lambda\sqrt{\omega})}\ e^{i\omega t} + \sum_1^\infty (-)^n\ \frac{2n^2\pi^2 j_2(n\pi r)}{n^2\pi^2 + i\omega\lambda^2}\ e^{-n^2\pi^2 t/\lambda^2} \quad .$$

APPENDIX E

NUMERICAL METHODS

We give here some details of the numerical procedure used to solve the equation of Bhatnagar, Gross, and Krook. Abbreviating it thus:

$$\frac{df}{dr} = G[r,f(r)], \qquad \text{(E-1)}$$

we may write the second-order predictor-corrector method (see, e.g., Hamming, 1962) as

$$f^*(r + h) = f(r) + h\, G[r,f(r)],$$

$$G^*(r + h) = G[r + h,\ f^*(r + h)],$$

$$f(r + h) = f(r) + \frac{h}{2}\{G(r) + G^*(r + h)\},$$

asterisks denoting predictor values. This method gave sufficient accuracy (a few %) with only ten steps between .1 and 1 A.U., so more elaborate methods were not needed.

f is a function of velocity as well as distance, and it is here that some care is needed. We use the characteristic coordinates $U,V_\perp$ introduced in section 2.3. The range of U extends to ∞. We must decide what finite range is to be included in the computation, and how many points to use to represent the function within that range. The form of f is Gaussian, with a peak near the bulk velocity. So the box, by which I mean the finite piece of velocity space that is included in the calculation, must be centered on the peak, and have dimensions of a few times the thermal speed. Now, in order to compute $G = \nu(f_B - f)$, f must be integrated over velocity; thus the criterion for choosing the step size, and the size of the box, is that the numerical integration

give accurate results. Experiment showed that a good size for the box was 6 (in the U direction) x 8 thermal speeds, with 16 x 32 mesh points.

Now, if there are no collisions, then f as a function of the characteristic coordinates $U,V_\perp$ is independent of r. Therefore, if the size of the box is properly adjusted (as described above) at r = D, then obviously it remains so for all r. Looked at in ordinary velocity variables $u,v_\perp$, the shape of the distribution function changes from spherical at r = D to cigar-shaped at the earth; and the shape of the box, by virtue of our peculiar coordinates, changes to match it. However, collisions cause a radical change in the distribution - it becomes much less elongated in one direction and much more so in the other, and no longer fits properly inside its box. Therefore, in the course of the calculation we keep a check on the parallel and perpendicular temperatures, and when the function starts to crowd towards one end of the box, or slop over the sides, we change the size of the box to fit it.

At each r, we compute the density n and mean velocity $\bar{u}$ of the gas, by integrating the distribution function. According to the continuity equation, $n\bar{u}r^2$ is independent of r. At each step in r, this product was calculated, as a check on the accuracy (it usually varied by less than 3%); then the density was adjusted to satisfy the continuity equation exactly (experience showed that the density was in greater need of correction than the velocity).

A complete solution (for one value of ν) took about a minute on the IBM 7094.

A program was devised to compute and plot the level curves of the distribution function. Figure 5 is an example of the results.

I should also explain why we cannot conveniently compute with a thermal velocity much greater than 1 percent of the bulk velocity. We are using characteristic coordinates, U, $V_\perp$, defined as the values of u, $v_\perp$ with which a particle would reach r = D if it were to travel there from its present position along a collisionless trajectory. But if $v_\perp$ is large enough, there may be no collisionless trajectory linking the particle to r = D (because orbits with large $v_\perp$ will mirror). So for sufficiently large $T_\perp$ the coordinate-system breaks down. Of course, if it were really necessary, one could use different coordinates, and work with higher temperatures.

REFERENCES

1. Beard, D. B., Planet, Space Sci. 14, 303-311 (1966).

2. Bernstein, I.B., and Trehan, S.K., Nuc. Fusion 1, 3-41 (1960).

3. Bhatnagar, P.L., Gross, E.P., and Krook, M. Phys. Rev. 94, 511-525 (1954).

4. Biermann, L., Brosowski, B., and Schmidt, H.U., Solar Phys. 1, 254-284 (1967).

5. Bigg, E.K., Nature 203, 1008-10 (1964).

6. Brandt, J.C., and Cassinelli, J.P., Icarus 5, 47-63 (1966).

7. Chandrasekhar, S., Revs. Modern Phys. 15, 1-89 (1943).

8. Chapman, S., and Cowling, T.G., "The Mathematical Theory of Non-uniform gases" (2nd Edition, Cambridge, U.P.) (1952).

9. Edmonds, A.R., "Angular Momentum in Quantum Mechanics" (Princeton Univ. Press) (1957).

10. Fano, U. and Racah, G., "Irreducible Tensorial Sets" (New York, A.P.) (1959).

11. Gold, T., "The Solar Wind" (Ed. Mackin and Neugebauer; Pergamon Press), 381-9 (1966).

12. Hamming, R.W., "Numerical Methods for Scientists and Engineers" (McGraw-Hill, N.Y.), 186 (1962).

13. Hundhausen, A.J., Asbridge, J. R., Bame, S.J., Gilbert, H.E., and Strong, I.B., J. Geophys. Research 72, 87-100 (1967).

14. Jokipii, J.R., Rand Memorandum RM 4714 NASA (1965).

15. Jokipii, J.R., Astrophys. J. 146, 480-7 (1966).

16. Longmire, C.L., "Elementary Plasma Physics" (Interscience-Wiley, N.Y.) (1963).

17. MacDonald, G.J.F., Revs. Geophys. 1, 305-49 (1963).

18. MacDonald, W.M., Rosenbluth, M.N., and Chuck, W., Phys. Rev. 107, 350-353 (1957).

19. Mathews, J., J. Soc. Indust. Appl. Math. 10, 768-80 (1962).

20. Neugebauer, M., and Snyder, C.W., J. Geophys. Research 71, 4469-84 (1966).

21. Northrop, T.G., Ann. Phys. 15, 79-101 (1961).

22. Parker, E.N., Phys. Rev. 107, 924-933 (1957).

23. Parker, E.N., Astrophys. J. 128, 664-76 (1958).

24. Parker, E.N., "Interplanetary Dynamical Processes" (Interscience-Wiley, N.Y.) 1963a).

25. Parker, E.N., Ibid, p. 137 (1963b).

26. Parker, E.N., Ibid, p. 78 (1963c).

27. Parker, E.N., Phys. Rev. 107, 924-933 (1957).

28. Parker, E.N., Astrophys. J. 128, 664-76 (1958a).

29. Parker, E.N., Phys. Rev. 109, 1874 (1958b).

30. Rosenbluth, M., "Magnetohydrodynamics" 57-66. (Lockheed Symposium, ed. Landshoff; Stanford Univ. Press)(1957).

31. Runcorn, S.K., Handbuch der Physik 47, Geophysik 1, 470-497 (1956).

32. Scarf, F.L., Wolfe, J.H., and Silva, R.W., J. Geophys. Research 72, 993-1005 (1967).

33. Shkarofsky, I.P., Johnston, T.W., and Bachynski, M.P., "The Particle Kinetics of Plasmas" (Addison-Wesley, Reading, Mass.) Ch. 2 (1966).

34. Smith, E.J., Davis, L., Jr., Coleman, P.J., Jr., and Jones, D.E., Science 149, 1241-2 (1965).

35. Sonett, C.P., Colburn, D.S., Currie, R.G., J. Geophys. Research 72, 5503-7 (1967).

36. Sytinskiy, A.D., Geomag. Aeron 6, 556-60 (1966).

37. Tozer, D.C., and Wilson, J., Proc. Roy. Soc., A296, 320-9 (1967).

38. Weber, E.J., and Davis, L., Jr., Astrophys. J. 148, 217-227 (1967).

39. Wolfe, J.H., Silva, R.W., McKibbin, D.D., and Matson, R.H., J. Geophys. Research 71, 3329-35 (1966).

40. Chew, G.F., M.L. Goldberger, and F.E. Low, Proc. Roy. Soc. A 236 112-118 (1956).